1-1-2003

Design optimization of hollow cylinders in pure rolling contact

Daniel John Johannsen
Iowa State University

Design optimization of hollow cylinders in pure rolling contact

by

Daniel John Johannsen

A thesis submitted to the graduate faculty

in partial fulfillment of the requirements for the degree of

MASTER OF SCIENCE

Major: Mechanical Engineering

Program of Study Committee:
Donald Flugrad, Co-major Professor
Abir Qamhiyah, Co-major Professor
Loren Zachary

Iowa State University

Ames, Iowa

2003

Graduate College

Iowa State University

This is to certify that the master's thesis of

Daniel John Johannsen

has met the thesis requirements of Iowa State University

Signatures have been redacted for privacy

TABLE OF CONTENTS

LIST OF FIGURES

LIST OF TABLES

LIST OF SYMBOLS

ψ	Angular width of contact patch
a	Inner radius
b	Outer radius **(Section 5.1 and 5.3 only)**
b	Length of cylinder **(Section 5.2 and 5.4 only)**
c	Outer radius **(Section 5.2 and 5.4 only)**
θ	Angle of location on cylinder
w	Linear contact patch width
K_D	Factor used in contact patch calculation
D_1	Diameter of one roller
D_2	Diameter of second roller
p	Force applied per unit length
E	Modulus of Elasticity
β	Unitless factor
q	Load factor
λ_n	Unitless factor
n	Counter for Taylor series
$(\sigma_r(\theta))_{a=0}$	Stress in direction of applied loading (solid roller)
$(\sigma_\theta(\theta))_{a=0}$	Bending stress (solid roller)
$(u(\theta))_{a=0}$	Displacement in direction of applied loading (solid roller)
ν	Poisson's Ratio
C	Unitless factor
D	Unitless factor
α	Ratio of ID to OD (unitless)
H_n	Unitless factor
H'_n	Unitless factor
L_n	Unitless factor
L'_n	Unitless factor
r	Radial location in cylinder
$\sigma_r(\theta)$	Stress in direction of applied loading
$\sigma_\theta(\theta)$	Bending stress
$u(\theta)$	Displacement in direction of applied loading
N	Normal load in loaded cylinder

$\mathbf{A}$	Cross sectional area of cylinder
$\mathbf{M_x}$	Moment in loaded cylinder
$\mathbf{A_m}$	Area integral
$\mathbf{R}$	Average radius of cylinder
$\mathbf{V}$	Shear force in cylinder
$\mathbf{P}$	Load applied to cylinder
$\mathbf{M_o}$	Moment factor
$\mathbf{p_{max}}$	Maximum Contact Pressure
δ	Displacement
$\mathbf{K^0}$	Stress Factor

1 INTRODUCTION

The advantages of using hollow rollers in loaded applications have been apparent for some time. Much of the research has been centered on the use of hollow rollers in roller bearings. Research in this area has shown hollow rollers to have advantages in accuracy of rotation and stiffness, even at high speeds [1].

A related area of interest is the use of hollow rollers in pure rolling contact with another roller. This situation differs slightly, as some benefits seen when using hollow rollers in a roller bearing are not seen when rollers are used in friction drives. One main advantage of using hollow rollers in a roller bearing is the additional sharing of load between rollers as the rollers deflect more than solid rollers do under the same load [2]. With only one set of rollers in contact the only reduction in stress available is seen when the area of contact between the rollers expands under load.

This situation where only one set of rollers is in contact is the one seen in most friction drive designs. One of the main disadvantages of friction drive systems compared to gear drive systems is the size required. The size of a friction drive system must be larger to account for the stress induced due to the normal force required to prevent slip. Using hollow rollers in a friction drive system can decrease the stresses in the rollers, thereby allowing smaller rollers to be used. A reduction in size would allow a friction drive design to be considered for space-sensitive applications where otherwise a gear drive would be necessary.

Hertz developed equations for solid members in contact with each other [3]. His equations work well for solid rollers but are not directly applicable to hollow rollers. The investigation done in this work is an attempt to develop an analytical method of determining the stresses expected to be seen in a loaded hollow roller, as Hertzian equations provide a method for loaded solid rollers.

In addition to the primary method of stress and displacement calculation, several methods of determining the stress in hollow rollers are used. These calculations are performed as a check against the accuracy of the primary method.

The primary method of determining the stresses is an analytical method using equations in series form.

The first comparative method involves a finite element analysis (FEA) approach. The FEA software provides a comprehensive analysis of the stresses throughout the cylinder being studied, and has many other pieces of information available as out also. However, this method of analysis is time consuming, as the problem set-up and computation time is fairly involved for each variation of cylinder geometry analyzed.

The second comparative method involves calculating stress in a hollow cylinder using equations developed for bending stress in a curved beam. This approach allows for only the computation of the bending stress, however.

Bending stress becomes a concern when using hollow rollers in an application where load is applied to them. Comparison between the bending stresses seen in rollers of varying hollowness (including completely hollow rollers) can be done using the primary analytical method as well as by finite element analysis. After determining the stresses through the volume, calculations can be performed to estimate the likely failure mode of a solid roller

design. Ideally, the design provides for equal likelihoods of failure from fatigue from bending stress and fatigue from contact stress.

2 PRIOR WORK

There are several published works dealing with loaded hollow cylinders. These papers are useful as a starting point for the subject of this work.

Bowen & Bhateja [1] write about optimizing the bearing preload and the hollowness of the rollers to provide the life, stiffness, and load capacity necessary for the design. Their work states, "excepting the slow speed applications, the load-life characteristic of the hollow roller bearing is usually determined by the bending fatigue life of the hollow rollers." In order to avoid failure by this mode in the application studied in this work, the thickness of the cylinder walls can be increased. This should change the problem to be more sensitive to contact stress and less sensitive to bending stress. Also in this work, the authors are able to calculate the compression of a hollow roller analytically and verify it experimentally.

Murthy & Rao [4] set out to provide an analytical method of calculating the contact stress in hollow cylinders in contact. Their method uses an equivalent modulus of elasticity, calculated by a method using the displacement of a hollow roller using the actual modulus of elasticity and the displacement of a theoretical solid roller with a modulus of elasticity adjusted to equate the two displacements. The equivalent modulus of elasticity is then used to calculate contact stress using the Hertzian equation for solid elements.

Zhao [2] studied, among other things, the effect of hollowness of the rollers in a roller bearing on the load profile on the race of the bearing. For this, he used finite element analysis. He found the expected lowering in the peak load value due to deformation of the

roller and allowance of more rollers to be in contact under load. This differs from the scenario of only 2 rollers in contact, as there are no more elements available to share load. He also comments on the difficulty of finding an analytical solution for hollow elements in contact - "For a solid roller bearing it seems easy to set up an analytical function of the load distribution, but for a hollow roller bearing it must be very difficult to do so, since the Hertzian assumption is unsuitable for such a multiply connected section." Also, he comments on the desirability of using hollow rollers, saying "Hollow roller bearings have many advantages, such as good flexibility, low contact stress, low shock loads, and excellent behavior in high-speed rotating."

Nelson [5] uses Taylor series expansions of equations given by Hertz (1881) to provide a practical analytical method of determining stress in the radial direction, bending stress and deflection throughout the volume of loaded hollow cylinders. This work is useful as his equations can be used to create an exhaustive analysis of the stresses and displacement.

Durelli and Lin [6] use Nelson's equations to provide a wide range of graphical results for cylinders of various degrees of hollowness. This is a useful paper as it provides a check on this author's use of Nelson's series equations.

3 SOLUTION APPROACH

The problem of determining the stresses and displacements in cylinders pressed together can be solved by multiple methods. Work was done using three methods.

3.1 Analytical Approach –Stress and Displacement via Nelson's Equations

Nelson's work gives equations in series form calculating stresses and displacements in hollow cylinders loaded by several different load profiles. His equations can be manipulated to give the stresses and displacements in the situation of cylinders pressing against each other. This is the primary aim of this work, to adapt Nelson's equations to this use and develop a fast, useful way to perform the calculations.

The geometry of the problem to be addressed numerically is shown in Figure 3.1. The assumption of symmetry in three directions allows for simplification of the calculations. This assumption should not affect the accuracy of the results, as different load profiles on the ends of the center two cylinders should have very minimal effect on the effects seen in the contact region between them. According to Saint Venant's Principle, "the difference between the stresses caused by statically equivalent load systems is insignificant at distances greater than the largest dimension of the area over which the loads are acting" [7]. This allows a simplified calculation using this assumption to be used for modeling an application where the center two cylinders are pressed together by various load profiles on the circumference opposite the contact area of interest. There are applications where a pair of

identical rollers is to be loaded by rollers of different diameters or even by a large ring with a concave surface in contact with one roller. The differing loading methods should not have great effect on the results found in the contact patch between the identical hollow rollers.

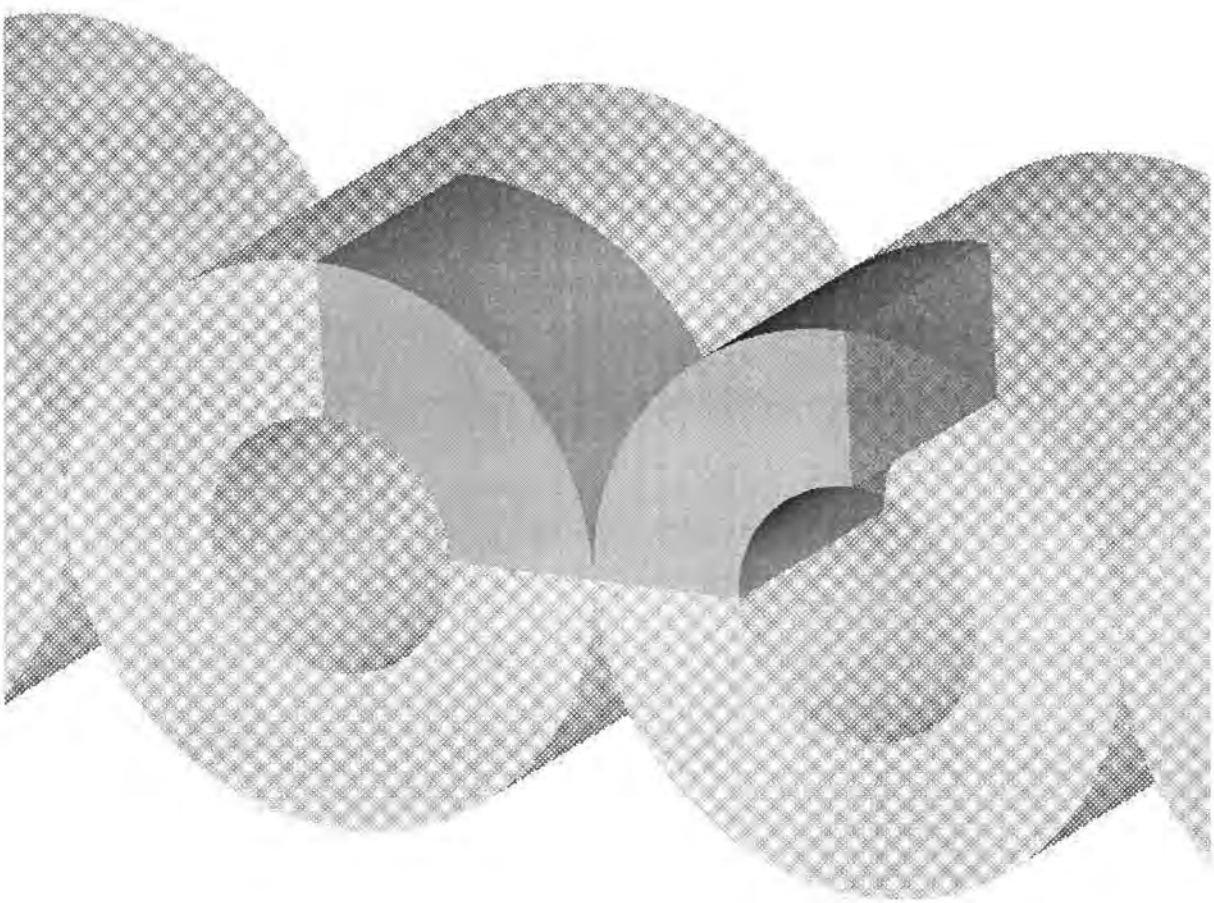

Figure 3.1, Simplified Geometry of Cylinders Pressed Together in Rolling Contact

Another assumption must be made to use Nelson's equations. The load distribution in the contact region to be analyzed must be assumed to be parabolic. This is a reasonable

assumption but may introduce some error into the solution. The validity of this assumption is analyzed in section 4.3. Figure 3.2 shows the parabolic load distribution, and also defines some of the variables used in the solution.

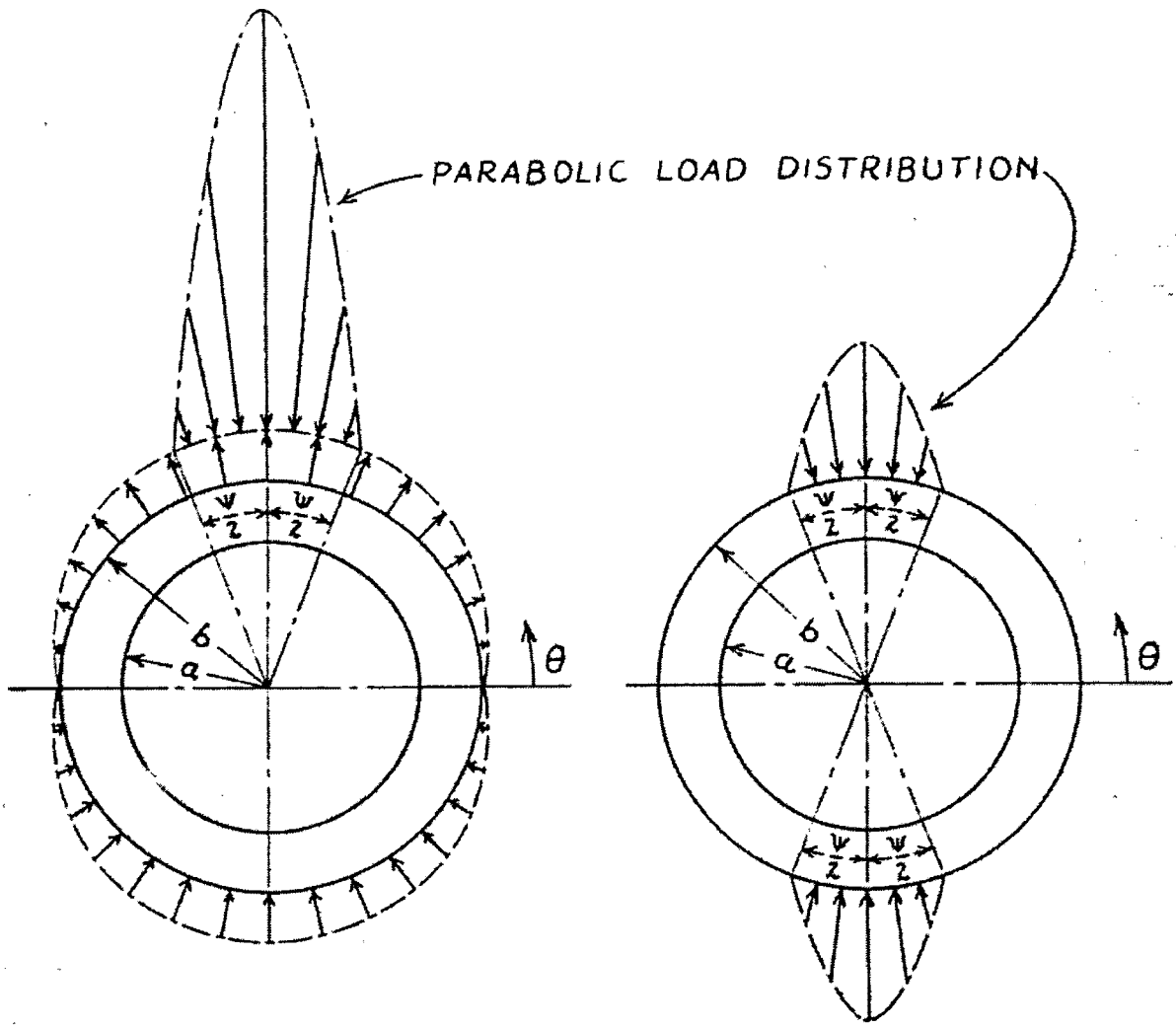

Source: Nelson, C. W., Stresses and Displacements in a Hollow Circular Cylinder. Ph.D. thesis, University of Michigan, 1939. [5]

Figure 3.2 Parabolic Load Distribution on Hollow Cylinder

The factor ψ shown in Figure 3.2 must be determined before Nelson's calculations can be performed. Although outside the scope of this thesis, work was done by the author showing the contact patch width differs only marginally from that of a solid cylinder in

cylinders with inner diameters less than 0.9 times the outer diameter. This finding is validated by the FEA results in section 4.3. Working with this assumption, the factor ψ can be calculated by a method used for a solid cylinder. Equation 3.2 below gives the length of the region of contact for two cylinders in contact [8]. Equation 3.1 defines the geometry factor K_D needed in the calculation. The variable p is load per unit length, and since the cylinders are identical, D_1 and D_2 are replaced by two times the outer radius of the cylinders in contact, b. The value w is the width of the contact patch, and E is the modulus of elasticity.

$$K_D = \frac{D_1 D_2}{D_1 + D_2} \quad (3.1)$$

$$w = 2.15\sqrt{\frac{pK_D}{E}} \quad (3.2)$$

The dimension w is a linear dimension, and is converted to the angular dimension ψ as follows. The factors band ψ are those shown in Figure 3.2.

$$\psi = \arctan\frac{w}{b} \quad (3.3)$$

A load factor used in Nelson's equations is the factor q. It is a factor with units of pressure, and is calculated as below.

$$q = \frac{3p}{2\psi b} \quad (3.4)$$

The factors calculated using the formulas below are used throughout the calculations. In the case of the calculation of λ_n, the integer n is used to produce an array that is then used in subsequent Taylor series calculations.

$$\beta = \frac{q\psi}{3\pi} \quad (3.5)$$

$$\lambda_n = \frac{24}{n^3\psi^3}\left[\sin\left(\frac{n\psi}{2}\right) - \frac{n\psi}{2}\cos\left(\frac{n\psi}{2}\right)\right] \quad (3.6)$$

The following equations give the stress and displacement in a solid cylinder. These values are needed later in the calculation of stress and displacement in the hollow cylinder. The variables θ and r are defined in Figure 3.2, and define the location in the cylinder being analyzed.

$$(\sigma_r(\theta))_{a=0} = -2\beta\left\{1 + \sum_{n=2,4,\ldots}^{\infty}(-1)^{\frac{n}{2}}\lambda_n\left[n\left(\frac{r}{b}\right)^{n-2} - (n-2)\left(\frac{r}{b}\right)^n\right]\cos(n\theta)\right\} \quad (3.7)$$

$$(\sigma_\theta(\theta))_{a=0} = -2\beta\left\{1 - \sum_{n=2,4,\ldots}^{\infty}(-1)^{\frac{n}{2}}\lambda_n\left[n\left(\frac{r}{b}\right)^{n-2} - (n+2)\left(\frac{r}{b}\right)^n\right]\cos(n\theta)\right\} \quad (3.8)$$

$$(u(\theta))_{a=0} = -2\beta\frac{r}{E}\left\{1 + \sum_{n=2,4,\ldots}^{\infty}(-1)^{\frac{n}{2}}\lambda_n\left[\frac{n}{n-1}\left(\frac{r}{b}\right)^{n-2} - \frac{n-2}{n+1}\left(\frac{r}{b}\right)^n\right]\cos(n\theta)\right\}$$
$$+ 2\nu\beta\frac{r}{E}\left\{1 - \sum_{n=2,4,\ldots}^{\infty}(-1)^{\frac{n}{2}}\lambda_n\left[\frac{n}{n-1}\left(\frac{r}{b}\right)^{n-2} - \frac{n+2}{n+1}\left(\frac{r}{b}\right)^n\right]\cos(n\theta)\right\} \quad (3.9)$$

The parameter α is of importance as it is used throughout this work as the measure of hollowness of the cylinders. As seen in the equation below, α is simply a ratio of the inner diameter to the outer diameter.

$$\alpha = \frac{a}{b} \quad (3.10)$$

The calculations in Nelson's work are performed using a series expansion. Several factors are needed at each value of n in the series, and their values are calculated as shown below.

$$H_n = n^2(1-\alpha^2)^2 + n\alpha^2(1-\alpha^2) + \alpha^2(1-\alpha^{2n}) \quad (3.11)$$

$$H'_n = n^2(1-\alpha^2)^2 + n(1-\alpha^2) + \alpha^2(1-\alpha^{2n}) \quad (3.12)$$

$$L_n = n(1-\alpha^2) + (1-\alpha^{2n}) \quad (3.13)$$

$$L'_n = n(1-\alpha^2) + \alpha^2(1-\alpha^{2n}) \quad (3.14)$$

The radial displacement, u, bending stress, σ_θ, and radial stress, σ_r, in a hollow cylinder loaded by a parabolic load like in Figure 3.2 are given by the following equations (the arbitrary constant D is taken as zero and the constant C is taken so as to make u=0 at $\theta=\pi/2$). The analysis can be done at any depth, r, and at any angle, θ.

$$\sigma_r(\theta) = (\sigma_r)_{a=0} - \beta\frac{\alpha^2}{(1-\alpha^2)}\left(1-\frac{b^2}{r^2}\right)$$
$$-\beta\sum_{n=2,4,\ldots}^{\infty}(-1)^{\frac{n}{2}}\frac{\lambda_n}{Q_n}\left[\begin{array}{l} nH_n\alpha^{2n-2}\left(\frac{r}{b}\right)^{n-2} - (n-2)H'_n\alpha^{2n-2}\left(\frac{r}{b}\right)^{n} \\ +nL_n\alpha^{2n}\left(\frac{r}{b}\right)^{-n-2} - (n+2)L'_n\alpha^{2n-2}\left(\frac{r}{b}\right)^{-n}\end{array}\right]\cos(n\theta) \quad (3.15)$$
$$+\beta\sum_{n=3,5,\ldots}^{\infty}(-1)^{\frac{n+1}{2}}\frac{\lambda_n}{Q_n}\left[\begin{array}{l} nH_n\alpha^{2n-2}\left(\frac{r}{b}\right)^{n-2} - (n-2)H'_n\alpha^{2n-2}\left(\frac{r}{b}\right)^{n} \\ +nL_n\alpha^{2n}\left(\frac{r}{b}\right)^{-n-2} - (n+2)L'_n\alpha^{2n-2}\left(\frac{r}{b}\right)^{-n}\end{array}\right]\sin(n\theta)$$

$$\sigma_\theta(\theta)=(\sigma_\theta)_{a=0}-\beta\frac{\alpha^2}{(1-\alpha^2)}\left(1+\frac{b^2}{r^2}\right)$$
$$+\beta\sum_{n=2,4,\ldots}^{\infty}(-1)^{\frac{n}{2}}\frac{\lambda_n}{Q_n}\begin{bmatrix} nH_n\alpha^{2n-2}\left(\frac{r}{b}\right)^{n-2}-(n+2)H'_n\alpha^{2n-2}\left(\frac{r}{b}\right)^{n} \\ +nL_n\alpha^{2n}\left(\frac{r}{b}\right)^{-n-2}-(n-2)L'_n\alpha^{2n-2}\left(\frac{r}{b}\right)^{-n}\end{bmatrix}\cos(n\theta) \quad (3.16)$$
$$-\beta\sum_{n=3,5,\ldots}^{\infty}(-1)^{\frac{n+1}{2}}\frac{\lambda_n}{Q_n}\begin{bmatrix} nH_n\alpha^{2n-2}\left(\frac{r}{b}\right)^{n-2}-(n+2)H'_n\alpha^{2n-2}\left(\frac{r}{b}\right)^{n} \\ +nL_n\alpha^{2n}\left(\frac{r}{b}\right)^{-n-2}-(n-2)L'_n\alpha^{2n-2}\left(\frac{r}{b}\right)^{-n}\end{bmatrix}\sin(n\theta)$$

$$u(\theta)=(u)_{a=0}+C\sin(\theta)+D\cos(\theta)$$
$$-\beta\frac{r}{E}\left\{\begin{array}{l}\frac{\alpha^2}{(1-\alpha^2)}(1+\frac{b^2}{r^2})+\sum_{n=2,4,\ldots}^{\infty}(-1)^{\frac{n}{2}}\frac{\lambda_n}{Q_n}\begin{bmatrix}\frac{n}{n-1}H_n\alpha^{2n-2}\left(\frac{r}{b}\right)^{n-2}-\frac{n-2}{n+1}H'_n\alpha^{2n-2}\left(\frac{r}{b}\right)^{n} \\ -\frac{n}{n+1}L_n\alpha^{2n}\left(\frac{r}{b}\right)^{-n-2}+\frac{n+2}{n-1}L'_n\alpha^{2n-2}\left(\frac{r}{b}\right)^{-n}\end{bmatrix}\cos(n\theta) \\ -\sum_{n=3,5,\ldots}^{\infty}(-1)^{\frac{n+1}{2}}\frac{\lambda_n}{Q_n}\begin{bmatrix}\frac{n}{n-1}H_n\alpha^{2n-2}\left(\frac{r}{b}\right)^{n-2}-\frac{n-2}{n+1}H'_n\alpha^{2n-2}\left(\frac{r}{b}\right)^{n} \\ -\frac{n}{n+1}L_n\alpha^{2n}\left(\frac{r}{b}\right)^{-n-2}+\frac{n+2}{n-1}L'_n\alpha^{2n-2}\left(\frac{r}{b}\right)^{-n}\end{bmatrix}\sin(n\theta)\end{array}\right\}$$
$$+\nu\beta\frac{r}{E}\left\{\begin{array}{l}\frac{\alpha^2}{(1-\alpha^2)}(1-\frac{b^2}{r^2})-\sum_{n=2,4,\ldots}^{\infty}(-1)^{\frac{n}{2}}\frac{\lambda_n}{Q_n}\begin{bmatrix}\frac{n}{n-1}H_n\alpha^{2n-2}\left(\frac{r}{b}\right)^{n-2}-\frac{n+2}{n+1}H'_n\alpha^{2n-2}\left(\frac{r}{b}\right)^{n} \\ -\frac{n}{n+1}L_n\alpha^{2n}\left(\frac{r}{b}\right)^{-n-2}+\frac{n-2}{n-1}L'_n\alpha^{2n-2}\left(\frac{r}{b}\right)^{-n}\end{bmatrix}\cos(n\theta) \\ -\sum_{n=3,5,\ldots}^{\infty}(-1)^{\frac{n+1}{2}}\frac{\lambda_n}{Q_n}\begin{bmatrix}\frac{n}{n-1}H_n\alpha^{2n-2}\left(\frac{r}{b}\right)^{n-2}-\frac{n+2}{n+1}H'_n\alpha^{2n-2}\left(\frac{r}{b}\right)^{n} \\ -\frac{n}{n+1}L_n\alpha^{2n}\left(\frac{r}{b}\right)^{-n-2}+\frac{n-2}{n-1}L'_n\alpha^{2n-2}\left(\frac{r}{b}\right)^{-n}\end{bmatrix}\sin(n\theta)\end{array}\right\}$$
(3.17)

In order to get the solution to the problem of the cylinder on the right side of Figure 3.2 superposition is used. The results of the equations given by Nelson give results for the cylinder on the left hand side of Figure 3.2. The results of the equations and the results of the

equations with the cylinder mirrored vertically are added together, resulting in the cancellation of the forces not of interest to the subject of this work.

The stresses in two directions, the bending stress and the radial stress, are then known. Because a plane strain condition exists in long rollers, once a long cylinder is assumed, plane strain calculations can be performed on stresses found in the center of the cylinder. In plane strain, the stress in the third direction can be calculated using the following equation [9].

$$\sigma_a = \nu(\sigma_r + \sigma_\theta) \quad (3.18)$$

The Von Mises stress can be calculated since the stresses in all three directions are known. The standard formula for Von Mises stress is given below [9].

$$\sigma_{vm} = \frac{1}{\sqrt{2}}\left((\sigma_\theta - \sigma_r)^2 + (\sigma_r - \sigma_a)^2 + (\sigma_a - \sigma_\theta)^2\right)^{1/2} \quad (3.19)$$

A Visual Basic program was created which handles all the above calculations. The design goal of achieving a geometry leading to a minimum Von Mises stress in the region of contact was also included in the program. The program iteratively searches for the ideal geometry given inputs such as outer diameter, length, material properties, and the load applied. The code for the Visual Basic program is found in Appendix A.

3.2 Analytical Approach – Bending Stress Assuming Point Load

One alternative approach to the problem is to assume a point load can approximate the force between the cylinders. In this situation we have straightforward equations available.

The bending stress distribution in a loaded curved beam is given by the formula below [10].

$$\sigma_\theta = \frac{N}{A} + \frac{M_x(A - rA_m)}{Ar(RA_m - A)} \quad (3.20)$$

This equation can be used for the case of a hollow cylinder. In this case, the area A is the area of the cross section through one side of the hollow cylinder. The radius R used in the formula is the average radius through the cross section. The factor A_m is the integral of 1/r with respect to A. The factor r again defines the depth location in the cylinder. Formulas for these three factors are given below. In this section, a is the inner radius of the cylinder, b is the length of the cylinder, and c is the outer radius of the cylinder.

$$A = b(c - a) \quad (3.21)$$

$$R = \frac{a + c}{2} \quad (3.22)$$

$$A_m = b \ln \frac{c}{a} \quad (3.23)$$

The factors V, N and M_x are applied loads at an angle relative to the angle where the load is applied. They are calculated as shown below.

$$V = \frac{P}{2} \sin\theta \quad (3.24)$$

$$N = \frac{P}{2} \cos\theta \quad (3.25)$$

$$M_x = M_0 - \frac{PR}{2}(1 - \cos\theta) \quad (3.26)$$

Using Castigliano's theorem and the total strain energy in a curved beam, the factor M_o needed to calculate the moment M_x can be found, and is simplified into the form given below.

$$M_0 = \frac{PR}{2}\left(1 - \frac{2A}{RA_m\pi}\right) \quad (3.27)$$

These formulas can be used to calculate the bending stress at any point on the cross section of a hollow cylinder. The formulas were programmed into an Excel spreadsheet to perform these calculations.

3.3 FEA Approach – Displacement and Stresses

An approach to the problem involving a finite element analysis of the contact between the subject rollers can be used to validate the calculated results obtained in the previous section. The problem set-up is identical, where there is three-way symmetry, allowing for one eighth of each cylinder to be included in the FEA, as seen in the figure below.

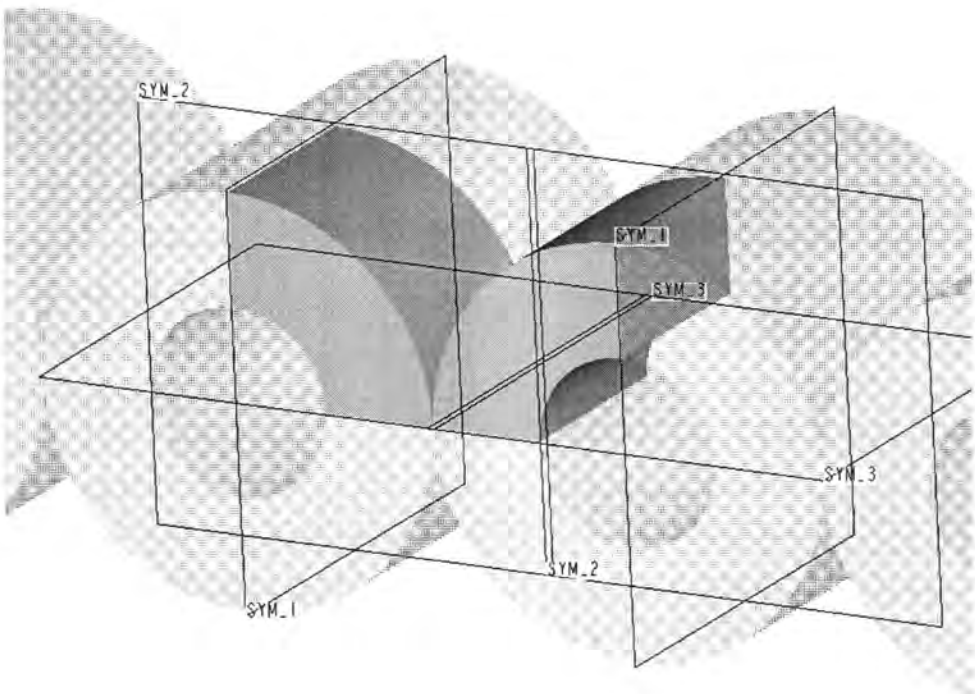

Figure 3.3, Simplification of Geometry for Simulation in FEA

In the figure above, the planes SYM_1, SYM_2, and SYM_3 are the planes about which the problem is symmetrical. On one face, the left-hand SYM_1, a displacement constraint is placed, forcing the left cylinder into the right one. On all other areas created when cutting away the symmetric material constraints are placed holding the nodes on those faces stationary within the plane. Motion in the other two directions is allowed.

Five geometries (α=0, α=0.45, α=0.6, α=0.754, and α=0.9) were analyzed using the FEA software ABAQUS. Below is the geometry of a cylinder with hollowness factor α=0.9

after a mesh was created, generating elements which together make up a representation of the original geometry.

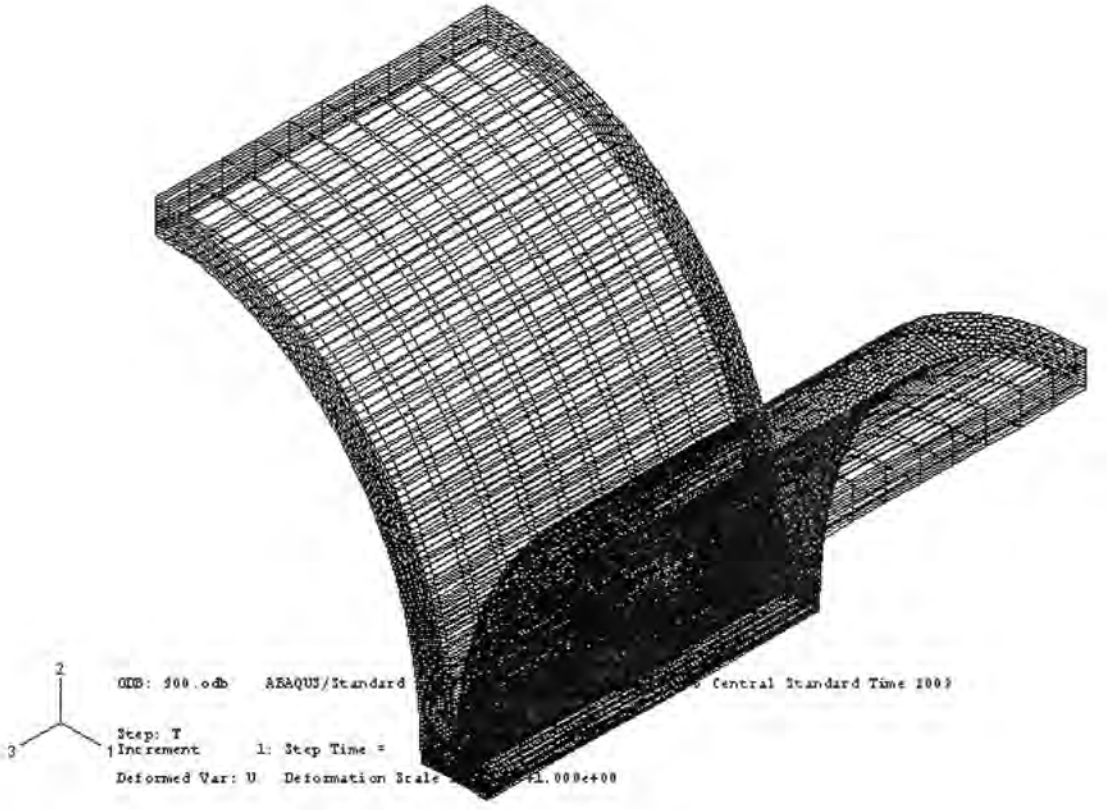

Figure 3.4, Meshed Representation of a Hollow Roller (α=0.9)

The figure below shows a closer look at the mesh created in the contact region of the cylinders.

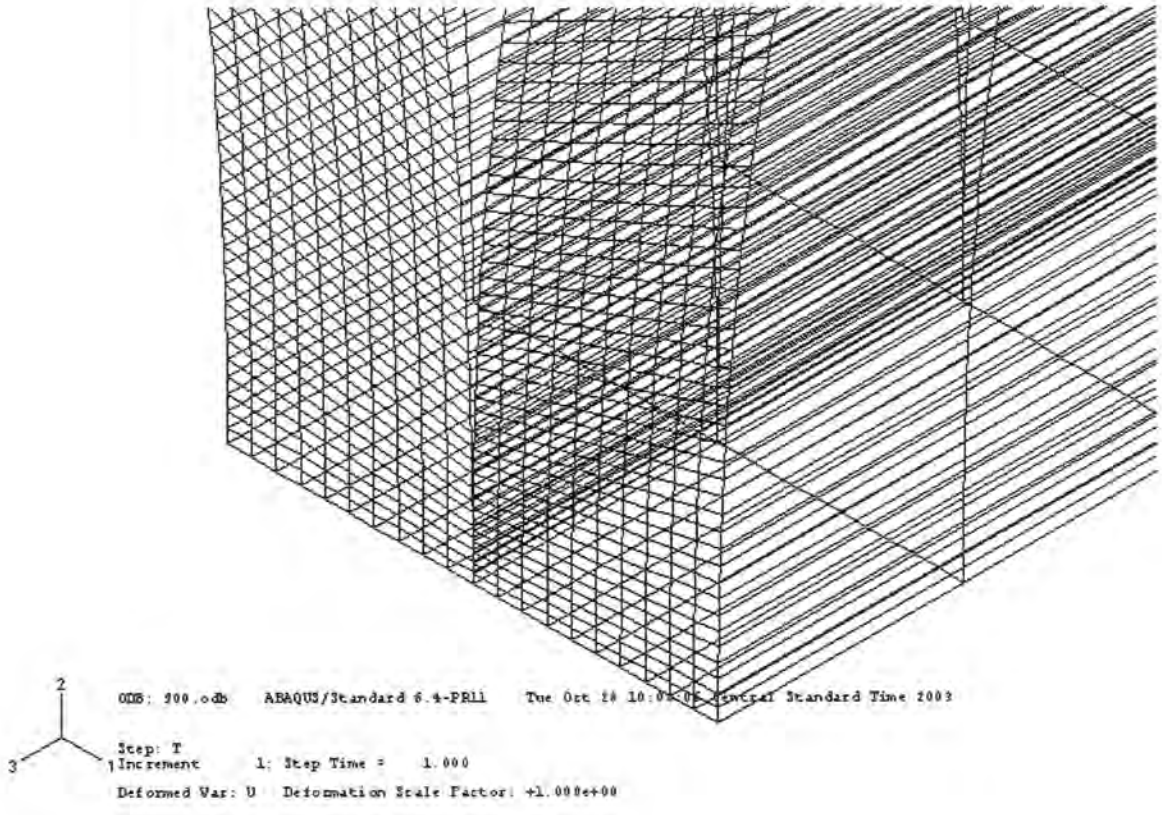

Figure 3.5, Contact Zone of Meshed Hollow Roller (α=0.9)

The geometry of the elements in the region of contact was forced to be the same in all cylinders with varying hollowness. This was important as it was seen that the mesh size and shape had a large effect on the ultimate results of the analysis. Illustrating this is the figure below showing the mesh in the contact region the most solid cylinder analyzed – the one with α=0.01.

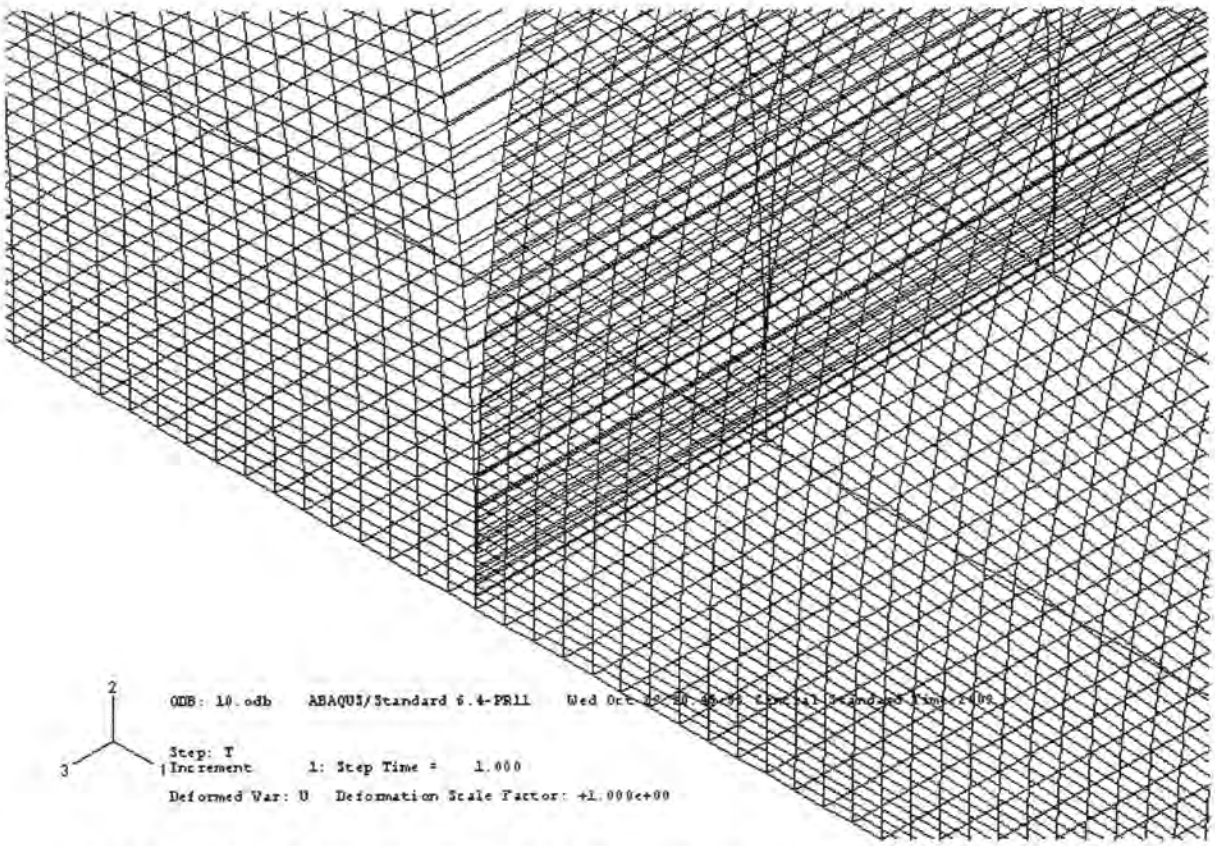

Figure 3.6, Contact Zone of Meshed Nearly Solid Roller (α=0.01)

In the analysis, the known quantity is a force pushing the cylinders together. To perform the analysis a displacement constraint is necessary since the distribution of load in the plane of symmetry isn't known. By forcing a displacement onto the place of symmetry at θ=0 the force on that plane is allowed to vary with location in the plane. However, this forces the user of the software to use an iterative approach to do an analysis with a given input force. This is done by first using an estimate of displacement for an initial FEA run. After the analysis is complete, the reaction forces on the nodes in that plane are output and compared to the intended input force. The analysis is iterated until the desired force is achieved. Through this iterative process a key piece of information is found – the movement of the centers of the cylinders toward each other when the cylinders are pressed together.

The displacement that is input into the analysis is exactly the displacement between centers of the cylinders.

3.4 Hertzian Calculations

In the case of a solid cylinder, the results of the FEA analysis can be checked using Hertzian calculations for comparison. The equation for the maximum load seen in solid cylinders pressed together is given below [11]. The variables below are those defined in section 3.2.

$$p_{max} = \frac{4P}{\pi wc} \quad (3.28)$$

If p_{max} is taken as a compressive principle stress, and the other two principle stresses are calculated as 2 times Poisson's ratio times the principle stress, the Von Mises stress can then be calculated.

The displacement can also be calculated using a Hertzian equation for a solid cylinder [11].

$$\delta = 4\frac{P}{b}\frac{\left(1-\nu^2\right)}{\pi E}\left(\frac{1}{3}+\ln\left(\frac{4c}{w}\right)\right) \quad (3.29)$$

4 RESULTS

4.1 Stresses Calculated via Nelson's Equations

The stresses in the radial and circumferential directions can be determined via Nelson's equations. This section gives results of calculations performed by the method of section 3.1. As described, the method uses a Visual Basic program to do the calculations. The Visual Basic program outputs results to Excel, allowing for further investigation and graphing of the results. Table 4.1 shows the values used in the Visual Basic simulation. The same input values are used in all calculation methods in Section 4, allowing for direct comparison of results.

Table 4.1, Table of Values Used in Calculations

Parameter	Description	Value
a	Inner radius	From 0.005 in. to 0.45 in.
b	Outer radius	0.5 in.
L	Length of cylinder	1 in.
P	Load per unit length applied	2000 lb/in.
E	Modulus of elasticity	$30*10^6$ psi
ν	Poisson's Ratio	0.3

Graphical results from the Visual Basic program make up the next several figures. In each graph, stress values resulting from the calculations are presented as stress factors. The

stress factor is defined in the equation below, where s is the stress of interest, P is the applied load, b is the outer radius, and c is the width of the cylinder.

$$K^0 = \frac{\sigma}{\left(\frac{P}{\pi bc}\right)} \quad (4.1)$$

The bending stress as calculated by Nelson's equations is shown below. The depth factor used in the plot is a normalized depth factor, z', defined as the ratio of distance down from the outer surface of the cylinder divided by the wall thickness. It can be seen that the bending stress is highly compressive near the point where load is applied ($\theta=-\pi$ and the depth factor, $z'=0$)

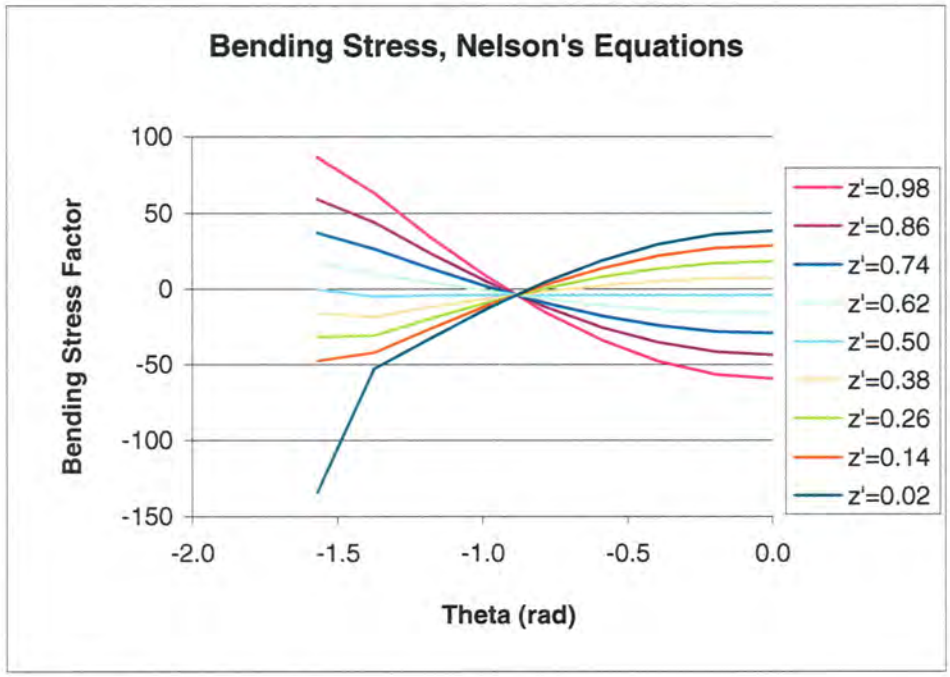

Figure 4.1, Bending Stress (α=0.754)

The next figure shows the stress in the radial direction. This stress is negligible except in the region near the point of load application. This is due to the effect of the contact stress.

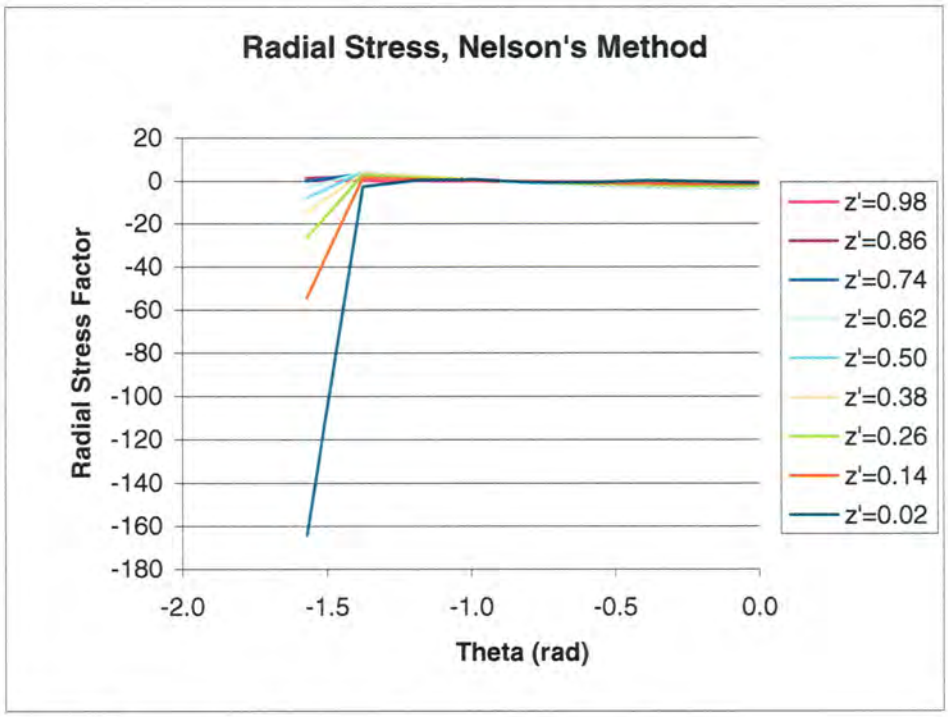

Figure 4.2, Radial Stress (α=0.754)

The following figure shows the axial stress in the simulated loaded cylinder. The stress seen in this direction is a combination of the radial and bending stresses, so except in the area near the point of load application the shape of the curves closely matches those of the bending stress curves.

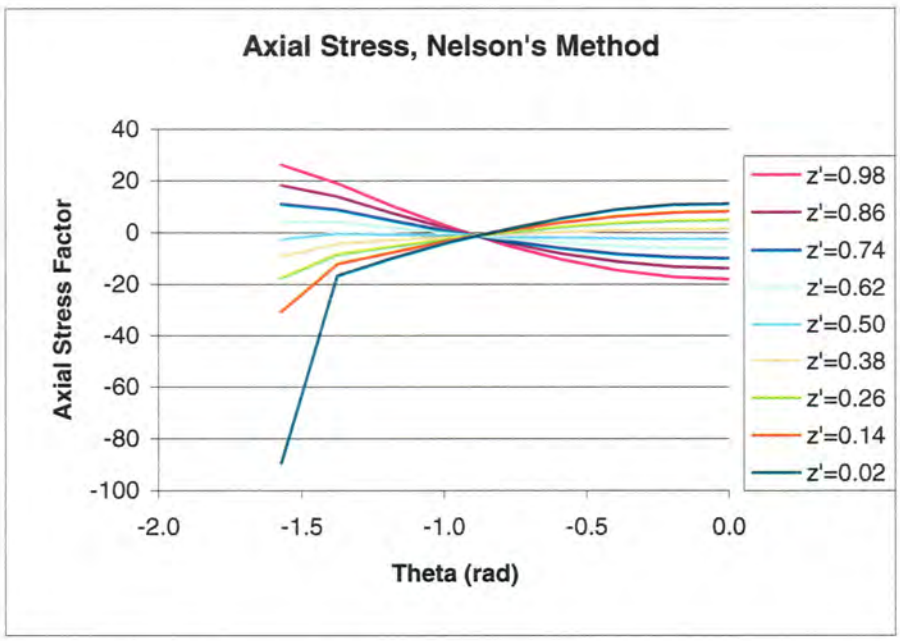

Figure 4.3, Axial Stress (α=0.754)

The Von Mises stress plot shown below is given as a contour plot. This is because the shapes of the curves on a two-dimensional plot were confusing. The Von Mises stress is a combination of the stresses in all three directions.

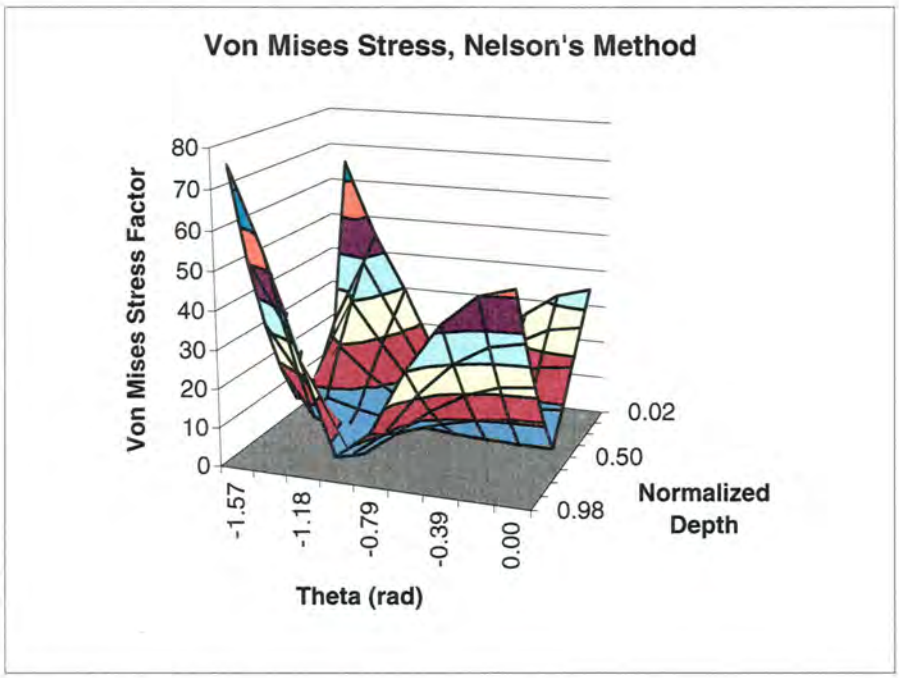

Figure 4.4, Von Mises Stress (α=0.754)

4.2 Stresses Calculated Assuming Point Load

The bending stress calculated using the equations for a point load applied to a cylinder, detailed in section 3.2, is useful as a comparison to the results achieved through Nelson's Equations. The input values used in the calculations involving Nelson's equations, given in Table 4.1, were used in these calculations as well. The calculations were performed in an Excel spreadsheet, and the results of the calculations are graphed below.

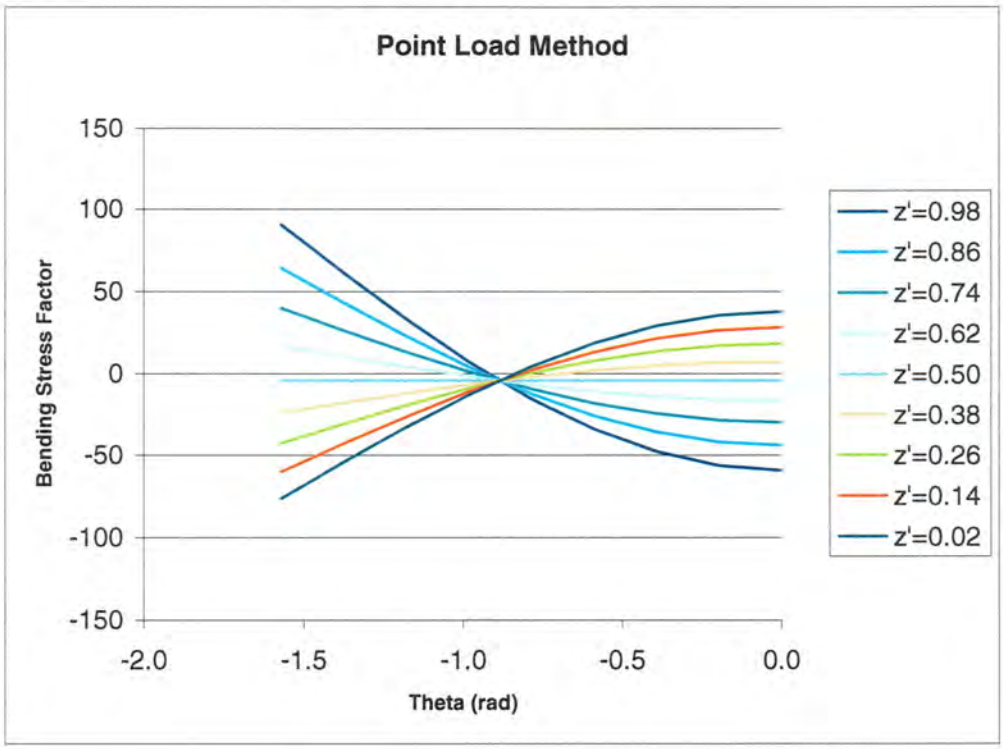

Figure 4.5, Bending Stress (α=0.754)

As expected, the stress is highest at the point of load application ($-\pi$) on the ID, and most compressive at the point of application on the OD. The reverse is true 90° from the point of load application (0°). The graph of bending stress above, when compared with the Figure 4.1, shows a difference at the OD at $-\pi$. The formulas for a point load do not take fully into account the peak in stress seen directly under the load.

4.3 Stresses and Contact Pressure Calculated via FEA

The results of the FEA are useful as a check against the previous results. The results can be treated with a great deal of confidence, as there are not as many assumptions necessary to make to perform the analysis. It was attempted to remove the effect the mesh has on the results by using a fine mesh and using the same mesh density for each cylinder configuration analyzed. Below are plots of Von Mises stresses garnered from the ABAQUS

analysis. The plane displayed in all plots is the plane of symmetry in the center of the cylinders being modeled because this is where a plane strain situation exists (see Figure 3.1, where the solid cylinder sections shown have the plane of interest in the center of the full cylinders facing away from the reader).

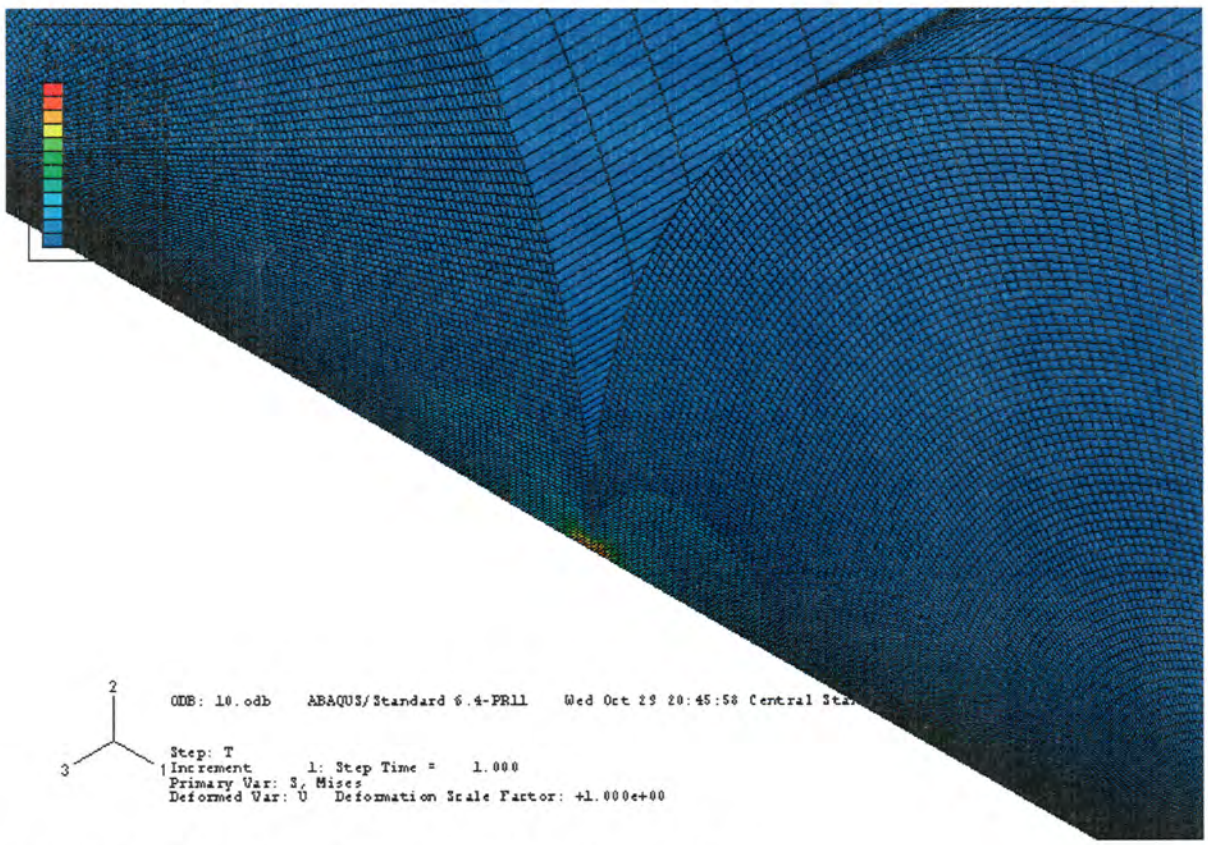

Figure 4.6, Von Mises Stress in Nearly Solid Cylinder (α=0.01)

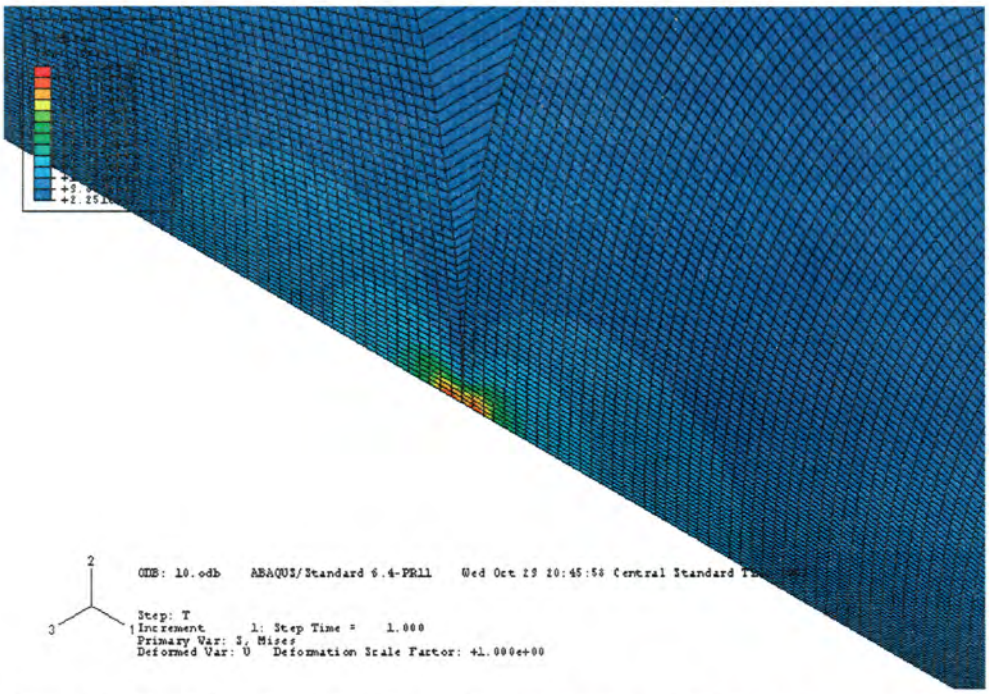

Figure 4.7, Von Mises Stress in Contact Zone of Nearly Solid Cylinder

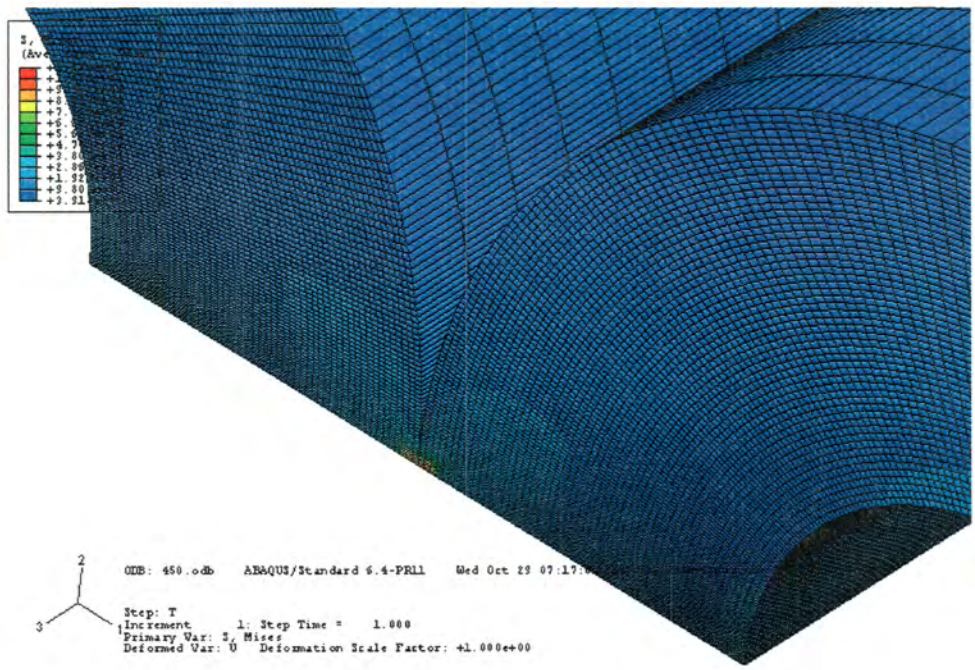

Figure 4.8, Von Mises Stress in Hollow Cylinder (α=0.45)

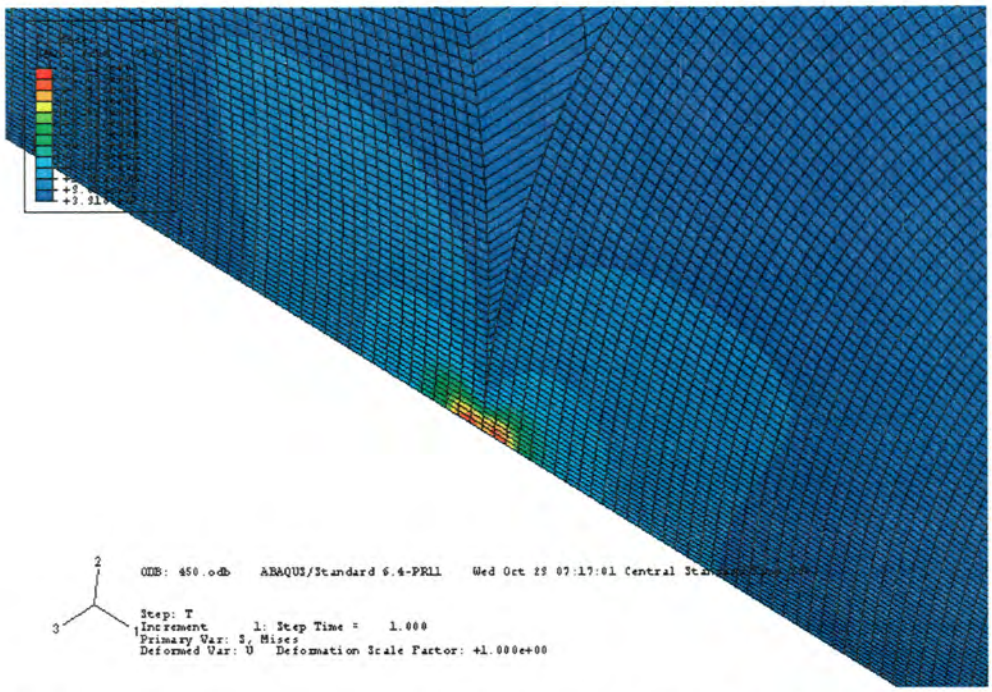

Figure 4.9, Von Mises Stress in Contact Zone of Hollow Cylinder (α=0.45)

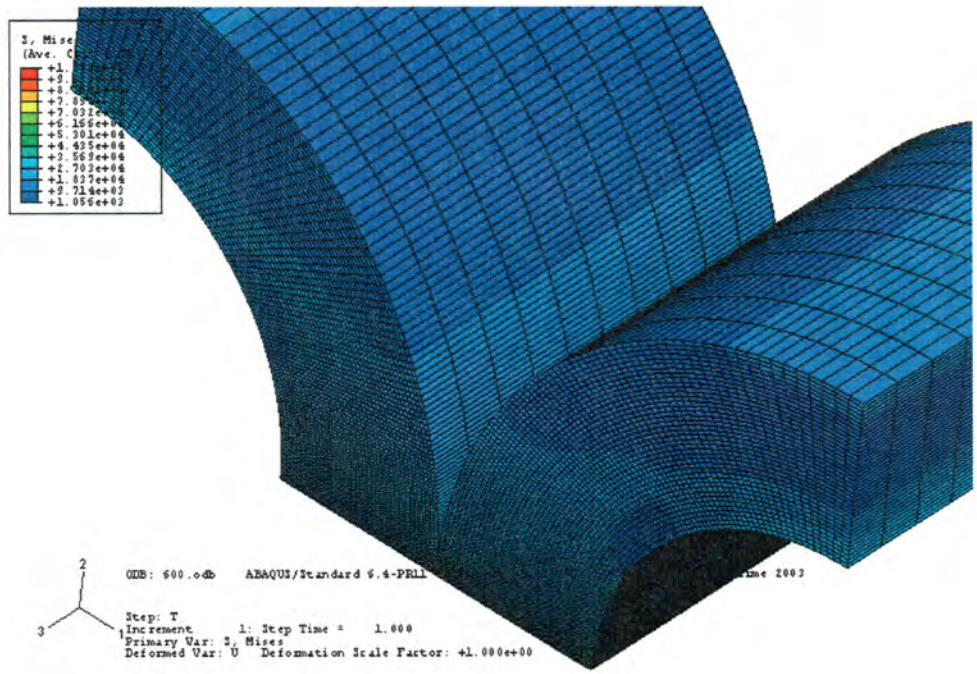

Figure 4.10, Von Mises Stress in Hollow Cylinder (α=0.6)

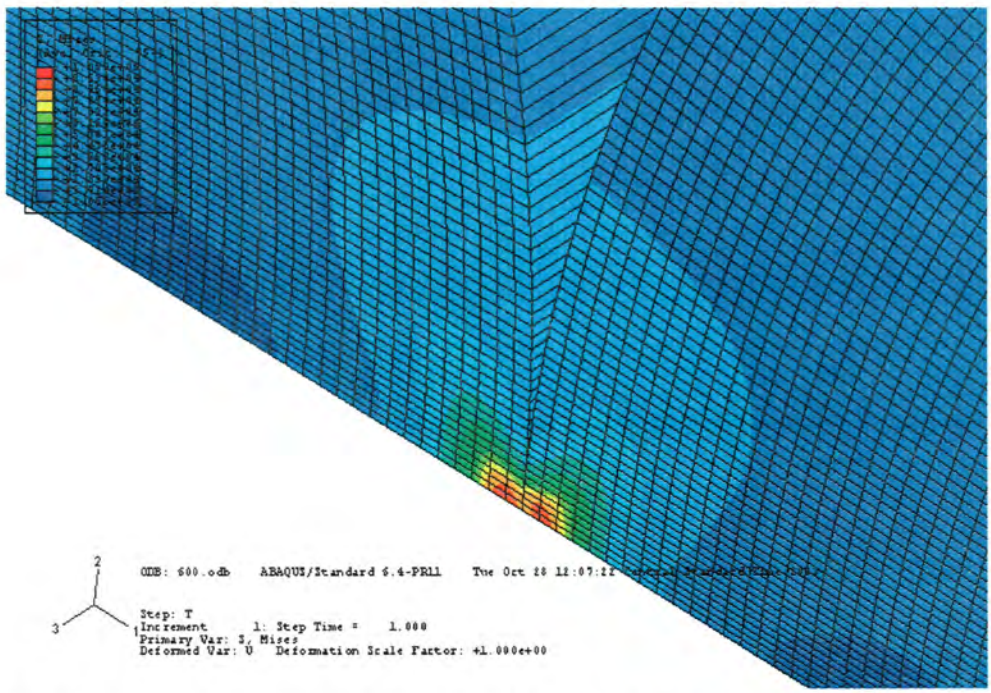

Figure 4.11, Von Mises Stress in Contact Zone of Hollow Cylinder (α=0.6)

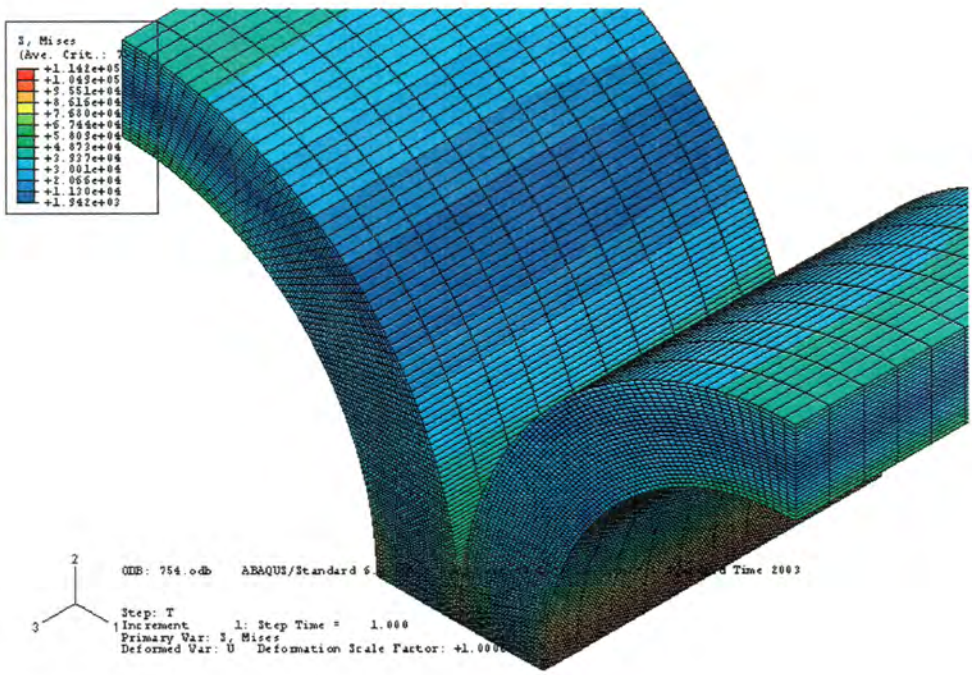

Figure 4.12, Von Mises Stress in Cylinder of Ideal Hollowness

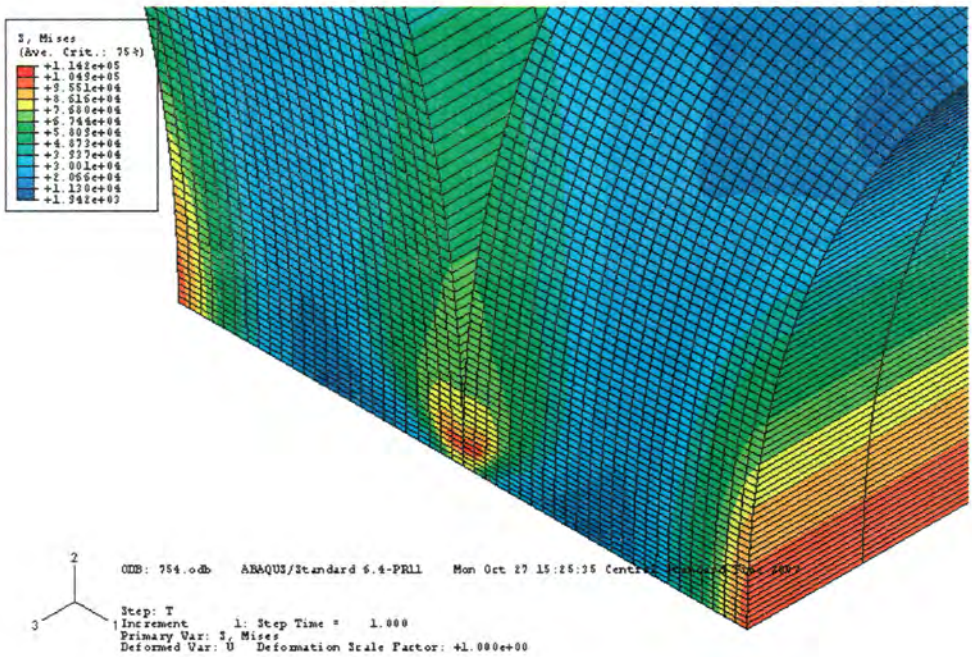

Figure 4.13, Von Mises Stress in Contact Zone of Cylinder of Ideal Hollowness

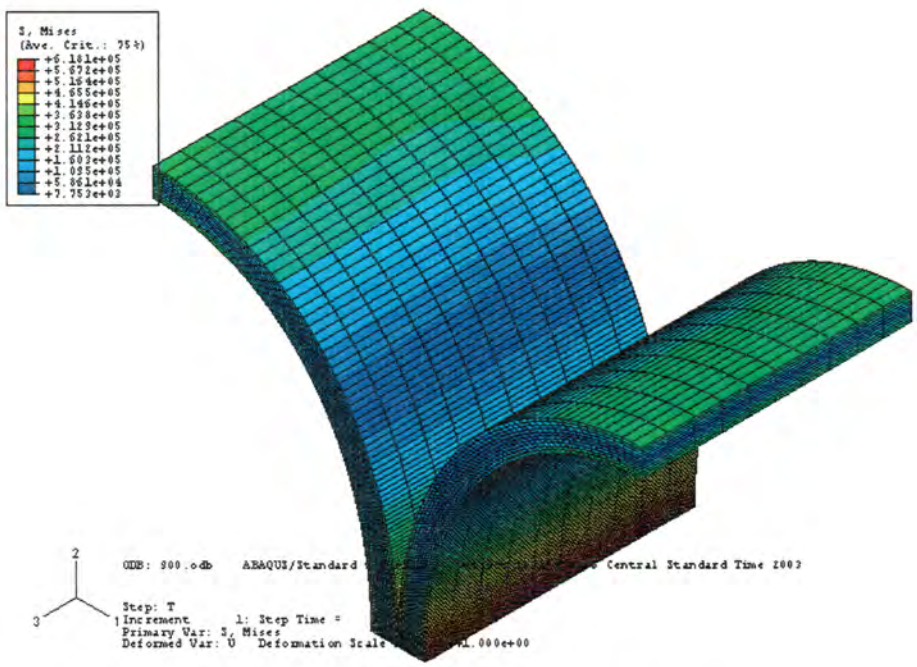

Figure 4.14, Von Mises Stress in Extremely Hollow Cylinder

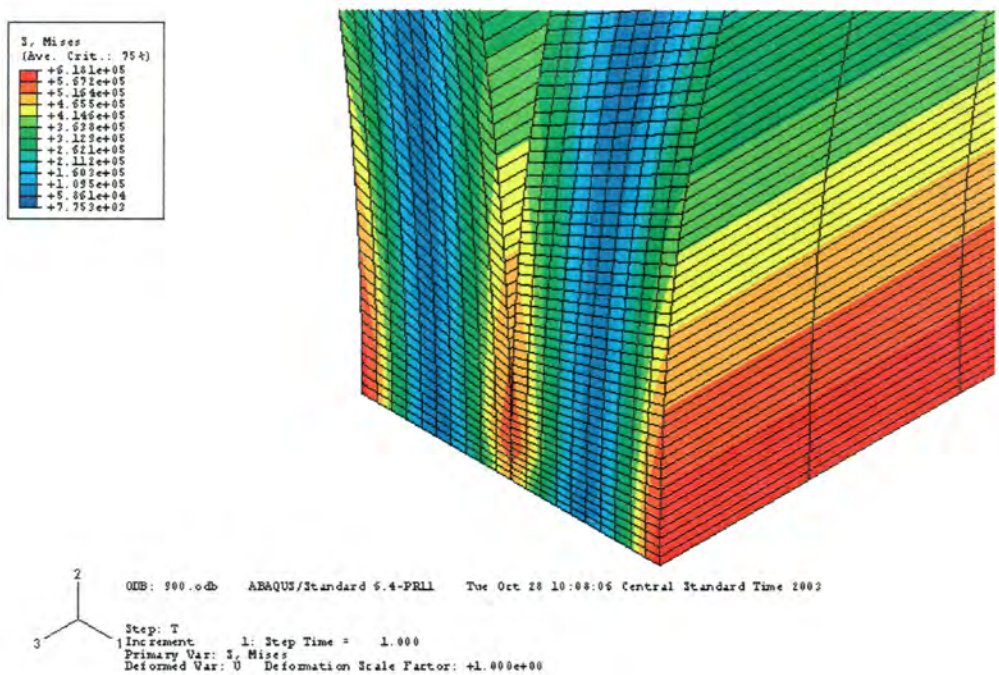

Figure 4.15, Von Mises Stress in Contact Zone of Extremely Hollow Cylinder

As in the case of Nelson's calculations, the Von Mises stress in the contact region is at a minimum at an intermediate value of hollowness. In the plot below, a 12% decrease in stress is seen at this intermediate hollowness (the exact stress values used to create the plot can be found in Appendix B). The graphs above also show a reduction in stress at the ideal hollowness, but due to the effect of the quickly increasing bending stress at ID of the cylinder the color scale is altered and the change in Von Mises stress is not easily seen. In the figure below the raw data output from the FEA was used to create a plot of Von Mises Stress in the contact region with increasing hollowness. The axes of the plot are adjusted to show only those data points with hollowness up to α=0.7. The stress factors seen in cylinders with high degree of hollowness are very high, and including only data from less hollow cylinders allows for clearer understanding of the change in Von Mises stress with hollowness.

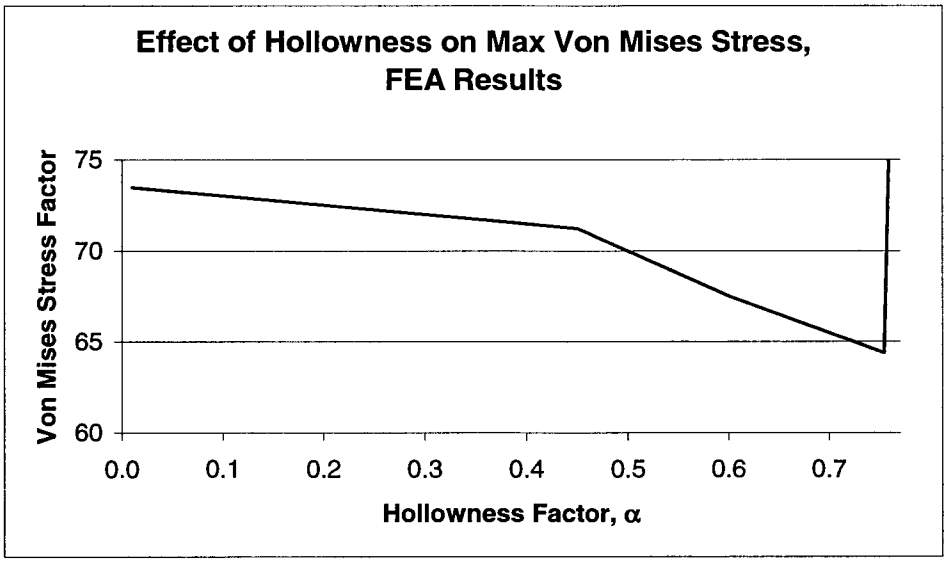

Figure 4.16, Von Mises Stress in Contact Region in FEA Results

As seen above, the minimum occurs at a value near α=0.75. The raw data used to create the above plot can be found in Appendix B.

A value of α =0.754 was used to further investigate the stresses in the FEA representation, as this was where the minimum Von Mises stress in the contact region occurred when simulated using Nelson's equations. Below are plots of stresses in all three directions in a cylinder with the ideal hollowness factor of α=0.754.

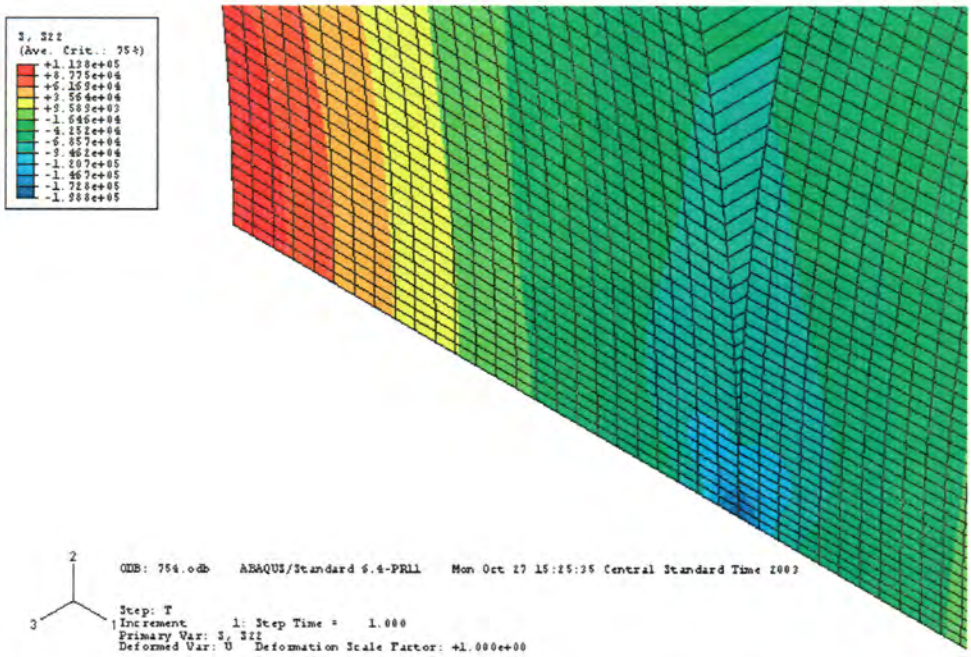

Figure 4.17, Bending Stress in Contact Region of Ideally Hollow Cylinder

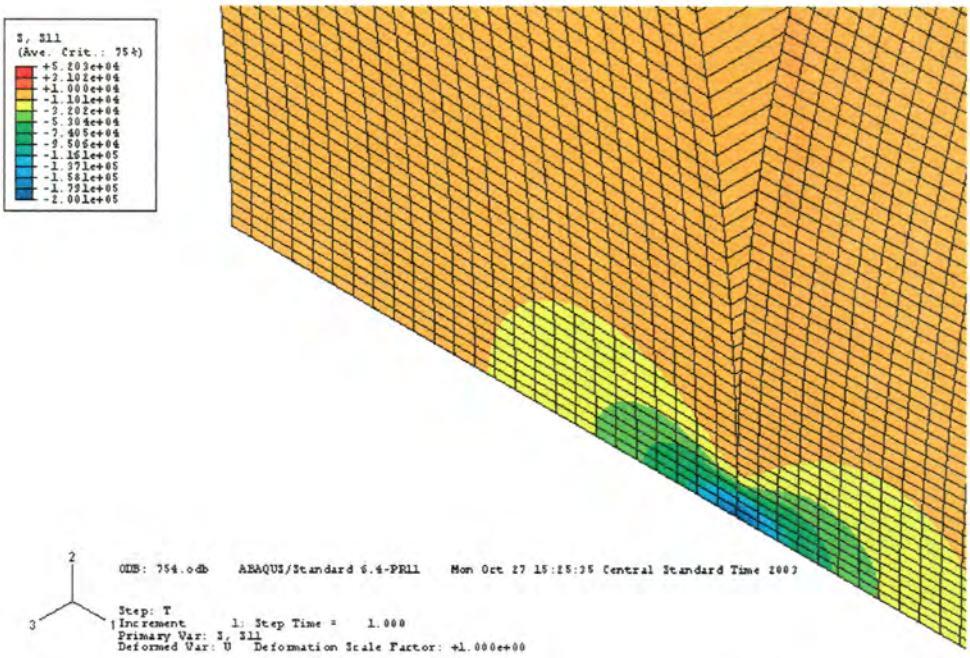

Figure 4.18, Radial Stress in Contact Region of Ideally Hollow Cylinder

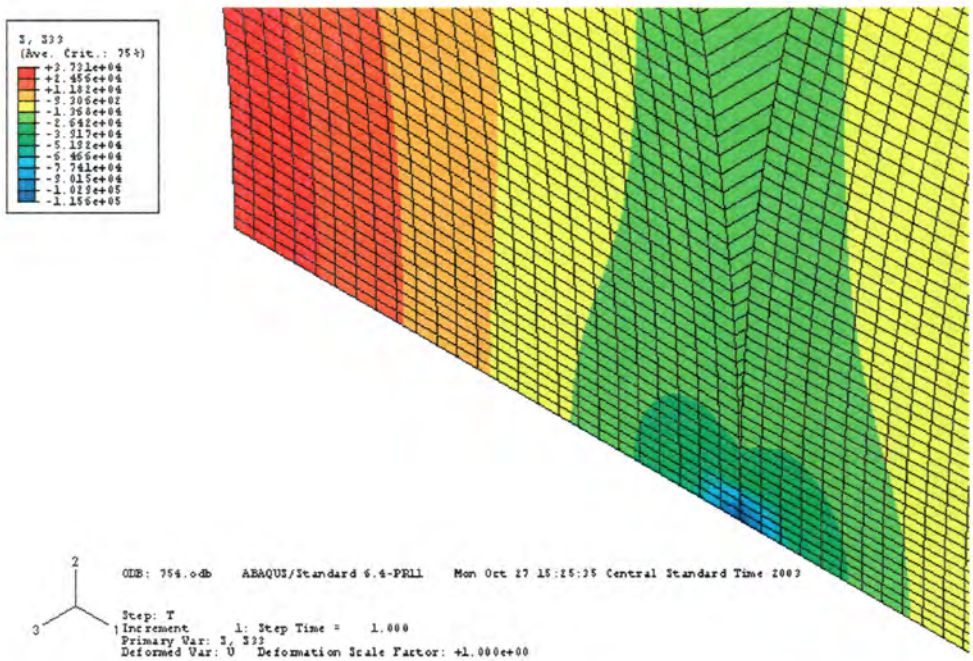

Figure 4.19, Axial Stress in Contact Region of Ideally Hollow Cylinder

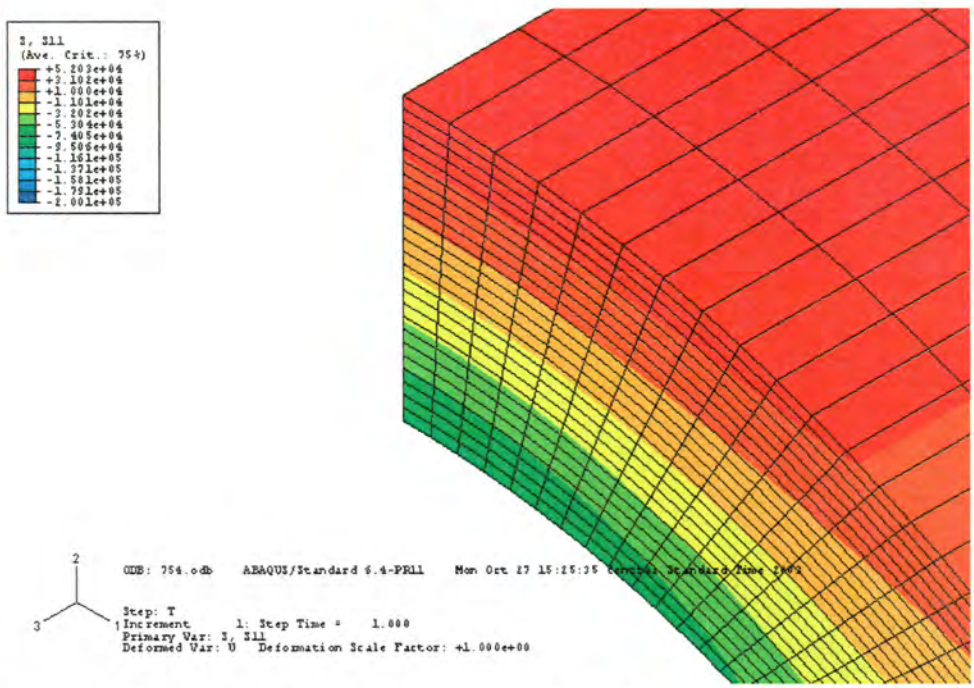

Figure 4.20, Bending Stress 90° from Contact in Ideally Hollow Cylinder

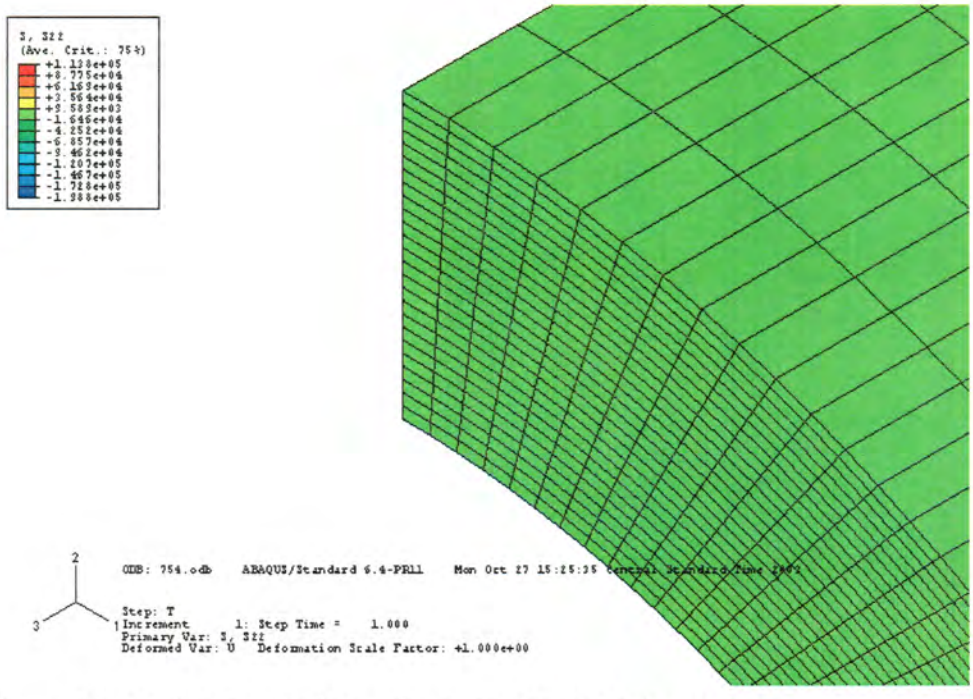

Figure 4.21, Radial Stress 90° from Contact in Ideally Hollow Cylinder

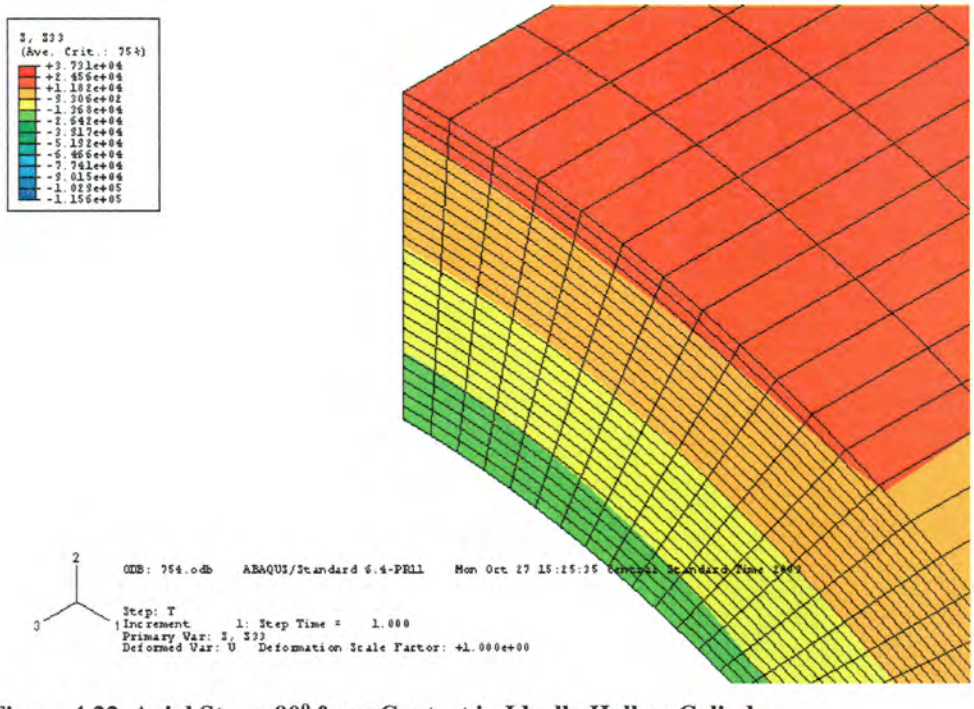

Figure 4.22, Axial Stress 90° from Contact in Ideally Hollow Cylinder

It is possible to output the contact pressure seen on the nodes in the contact region in the analyses of the cylinders of different hollowness. This is important as it can both validate the assumption of a constant contact patch size as hollowness increases up to α=0.9, and it can validate the assumption of a parabolic pressure distribution used in Nelson's equation derivation. The figure below shows the contact pressure of the different FEA runs, along with curves of parabolic shape for comparison. The normalized distance shown along the x-axis is the distance divided by the outer radius of the cylinder. The contact pressure factor is calculated in the same method as the stress factor except with pressure replacing stress in equation 4.1.

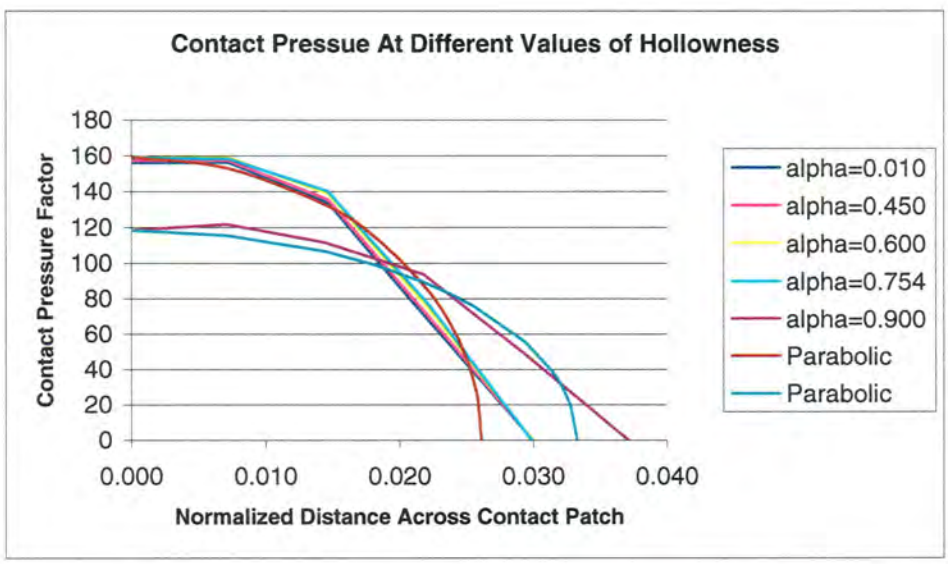

Figure 4.23, Contact Pressure in Contact Patch of Various FEA Models

As shown above, the pressure distribution varies only slightly in cylinders of low or moderate hollowness. Also, the pressure distribution does not vary greatly from a parabolic shape. The shape of the curve generated in each FEA model can vary greatly at the point where it reaches the X-axis. The distance between nodes of the mesh leads to some

uncertainty as to where the contact pressure reaches zero in the cylinder the FEA model represents. The location where the contact pressure reaches zero in the data set farther from the center of the load than the point where the contact pressure actually reaches zero would be. The point where it would reach zero is actually somewhere between the x value of that data point and that of the previous node. This is why the parabolic curves plotted for comparison in Figure 4.23 were created with x intercepts less than those of the FEA curves.

4.4 Displacement Calculated via Nelson's Equations and FEA

The displacement found by Nelson's equations and those found in the FEA runs are plotted in the figure below. The normalized displacement on the y-axis is the displacement divided by the outer radius of the cylinder.

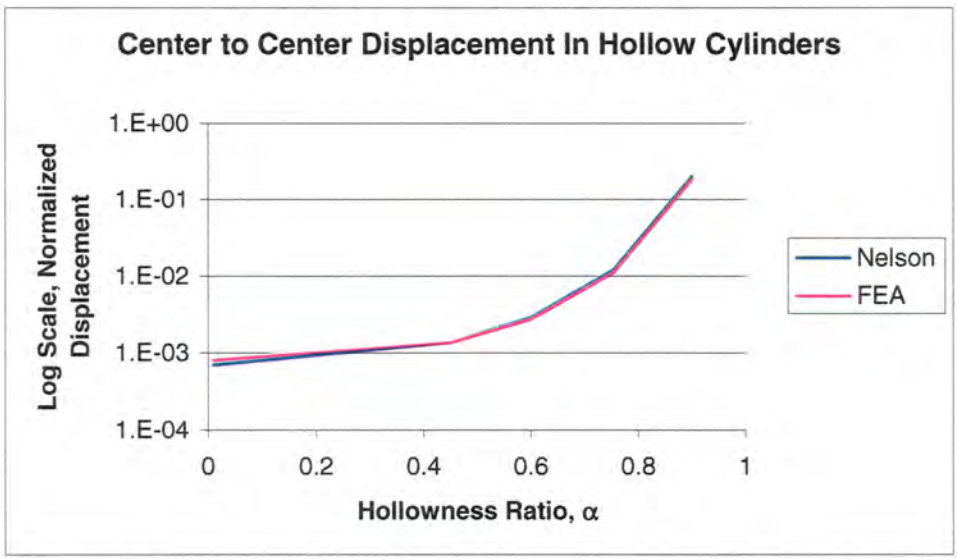

Figure 4.24, Center-to-Center Displacement via Nelson's Equations and FEA

As the plot shows, the rate of displacement increases greatly as the hollowness increases. The accuracy of both methods can be judged to be good due to the replication of results between them. As can be seen in the data in Appendix B, there is less than 16% difference between the methods at each of the hollowness values.

4.5 Hertzian Stress and Displacement – Solid Cylinder

The results of the calculations performed using Hertz contact stress equations show the validity of the FEA calculations. Below is the Excel spreadsheet used to do the calculations, with results outputted from the FEA run of nearly solid cylinders in contact.

Table 4.2, Hertzian Calculations and FEA Results

	Analytical	FEA	Units
r	0.5		in
v	0.3		
E	30000000		psi
P	2000		psi
c	1		in
K_d	0.25		in
w	0.0088		in
p_{max}	290120		psi
σ_1	-290120		psi
σ_2	-174072		psi
σ_3	-174072		psi
σ_{vm}	116048	105100	psi
ΔD_2	0.000445	0.000423	in

As the table shows, the results of the Hertzian calculations very nearly match those of the FEA. This adds credence to the methods used to determine the stress and displacement in cylinders in contact.

5 CONCLUSIONS AND FUTHER RESEARCH

The data resulting from the different methods of acquiring an understanding of the stresses and displacements in a loaded hollow roller supports the viability of the method developed – using a computer program to calculate the ideal geometry for the cylinder using Nelson's equations. Using finite element analysis to this end is also shown to be useful; however, the ease of use of the Visual Basic program developed by the author makes the tedious task of doing FEA runs for several geometries unnecessary.

The following figure illustrates the high level of correspondence between the results of all three methods used to calculate the bending stresses in hollow cylinders. This figure shows only the results of the analysis of a cylinder with the ideal hollowness, but similar correspondence is seen at various hollowness values chosen.

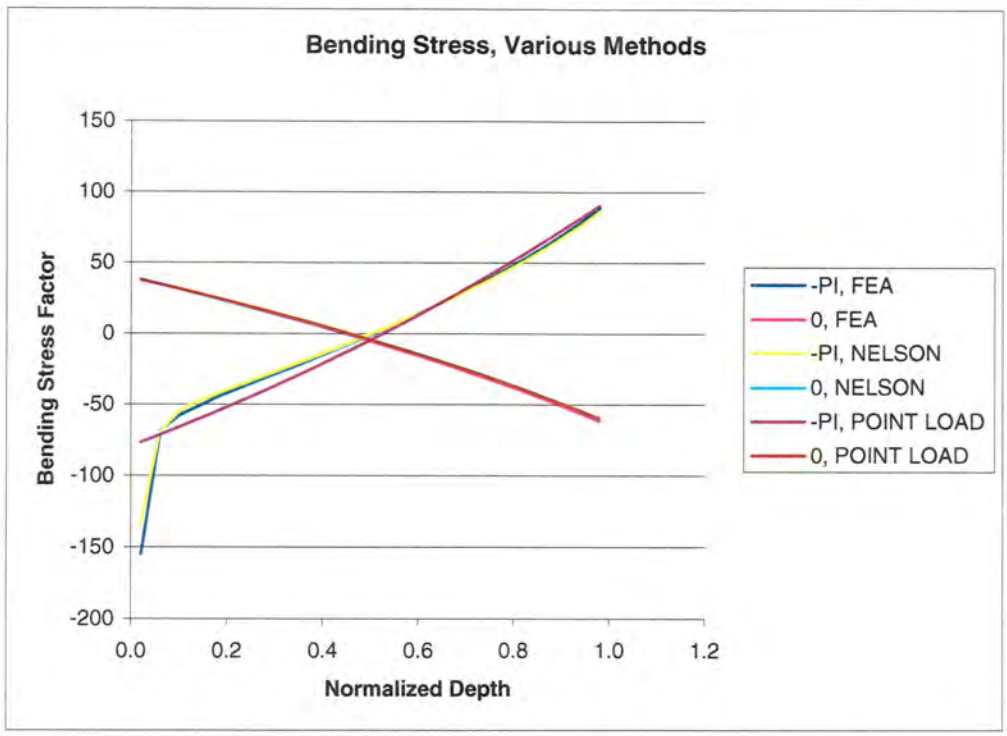

Figure 5.1, Bending Stress, all Three Methods (α=0.754)

Another area of interest is the balance between bending and contact stress. When replacing a solid roller in a mechanism with a hollow one, one must consider the change in failure mode. Solid rollers in rolling contact generally fail due to Hertzian stresses just below the surface. Hollow rollers have the possibility of fatigue failure due to bending stresses. These bending stresses have a maximum on the bore surface – the ID. A balance must be found that optimizes the life of the cylinders by attempting to have the cylinder fail by both modes simultaneously. This work concentrates on the optimization of cylinder geometry in order to prevent failure at the OD of the cylinder. However, additional work needs to be done in order to determine if the optimum design might need to be less hollow than predicted by the method of this work in order to prevent failure at the ID of the hollow cylinder due to

excessive tensile bending stress. The figure below shows the trend of the maximum bending stress in the cylinder increasing with increasing hollowness.

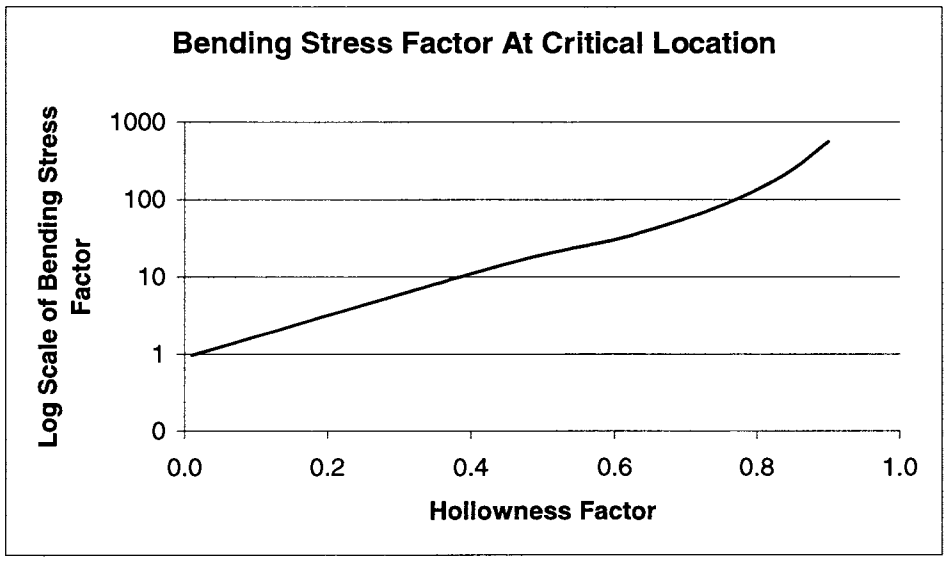

Figure 5.2, Bending Stress, Calculated Via Nelson's Equations

As well as the component of stress defined as bending stress seen in Figure 5.1, the other two directional components of the stress seen in the hollow cylinder by both Nelson's equations and FEA can also be compared individually. The following graphs allow for this comparison.

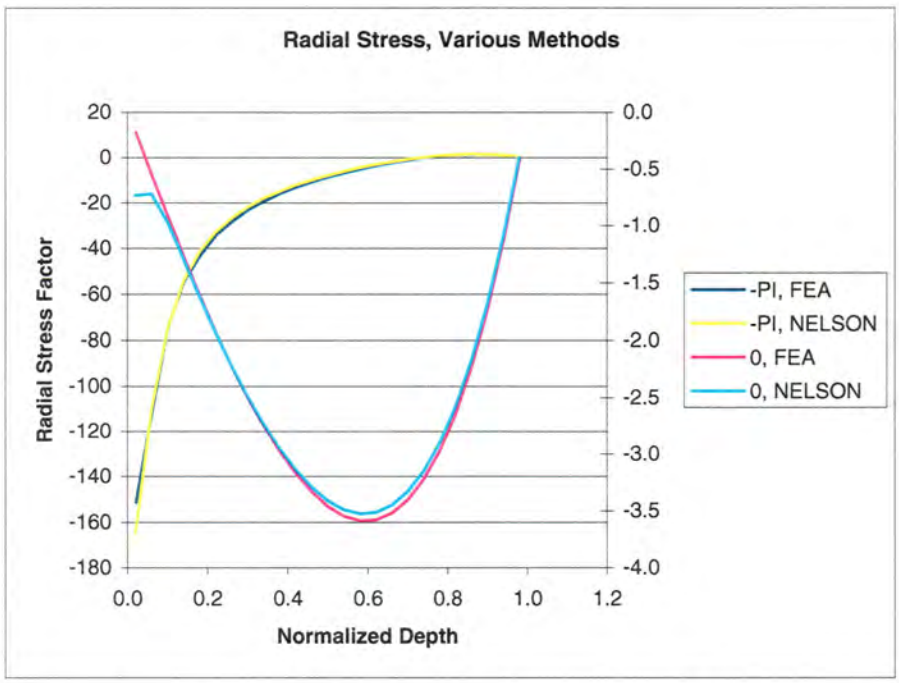

Figure 5.3, Radial Stress, FEA and Nelson's Equations (α=0.754)

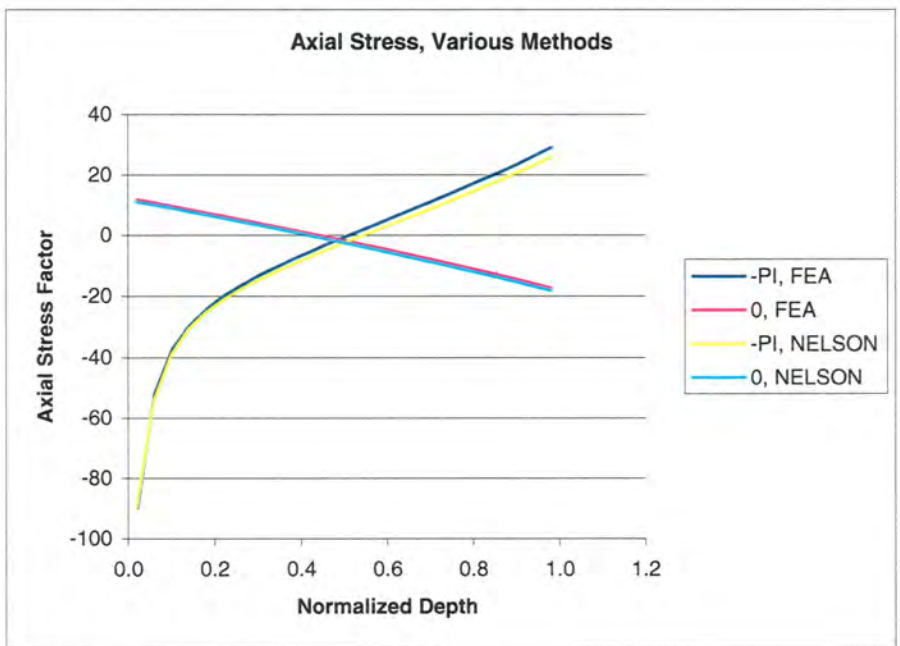

Figure 5.4, Axial Stress, FEA and Nelson's Equations (α=0.754)

An important thing to know when analyzing a hollow cylinder is the Von Mises stresses seen throughout its volume. Both through FEA and through using Nelson's equations it is possible to determine the Von Mises stresses at any point in the cylinder that is in plane strain. Both methods' results are shown below on the same plot, for comparison.

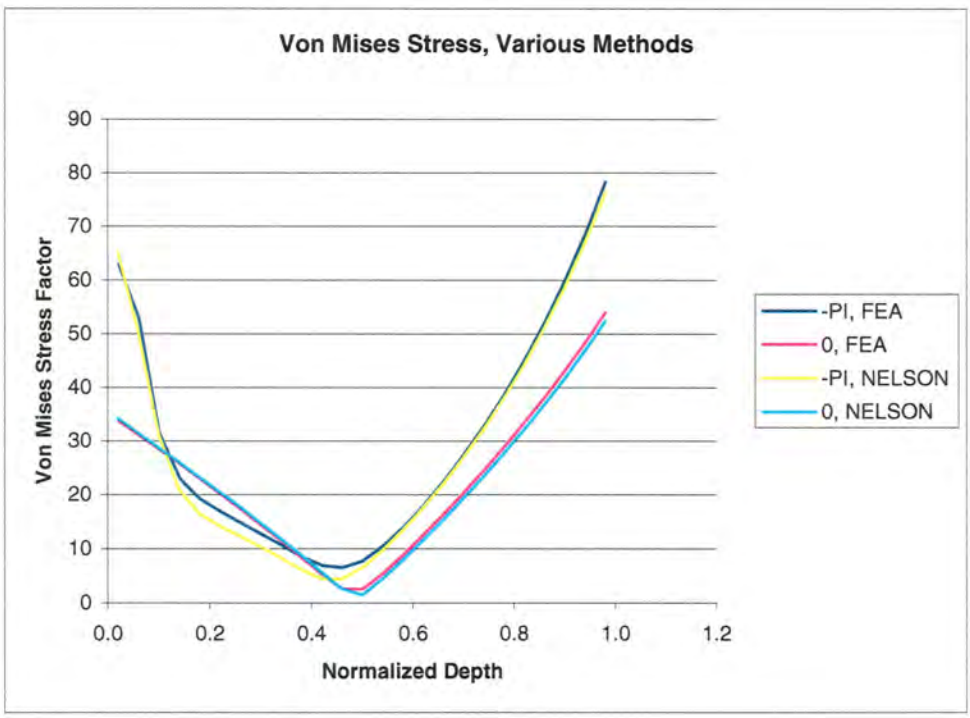

Figure 5.5, Von Mises Stress, FEA and Nelson's Equations (α=0.754)

The plot above shows very good correspondence between the two methods. It also shows where the points are which become critical when the cylinder is loaded. At the ID, when the normalized depth is 1.0, the Von Mises stress is at the maximum. As can be seen in Figure 5.1, Figure 5.3, and Figure 5.4, the dominant component of the stress at that point is the bending stress. At the OD (normalized depth equals 0.0) the Von Mises stress is also high. In cylinders of lesser hollowness this is the point of maximum Von Mises stress, but with this value of hollowness factor it is less than that seen at the ID. The stresses at this

point are all compressive, and because of their relatively equal magnitudes at this particular value of hollowness the Von Mises stress is at a minimum compared to the same point on the OD of cylinders of hollowness both greater and less than this "ideal" cylinder. This trend can be seen in the following graph, and the two methods of calculating the Von Mises stress at that point on cylinders of varying hollowness can be compared.

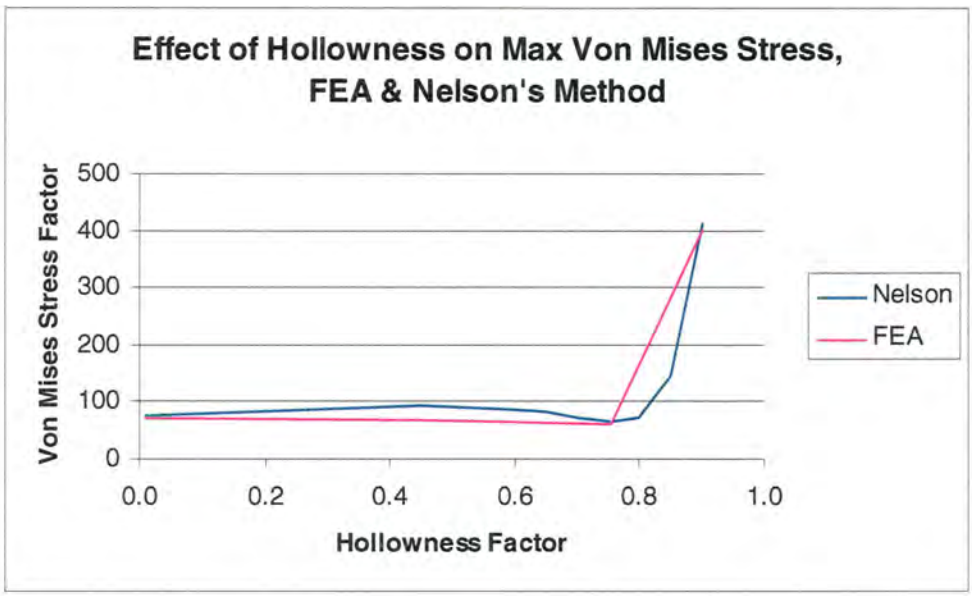

Figure 5.6, Maximum Von Mises Stress for Varying Hollowness

It was seen that the stresses in all three directions increase in magnitude with increasing hollowness. For this to result in Von Mises stresses following the curve above seems at first a bit paradoxical. However, because these stresses at the minimum point are all of the same sign, in this case compressive, the Von Mises stress can be reduced when the magnitudes of the stresses become closer in magnitude. The Von Mises stress is a measure of the distortion energy seen by the material. As the material is compressed from all

directions, the material does not tend to distort as it would if the stress were seen in only one or two directions.

Figure 5.6 illustrates the crux of the work done. Two methods of finding an optimum geometry for the cross section of a hollow cylinder to be loaded by a cylinder of identical size are validated by the similar results they produce. More importantly, one of the methods is a useful one that can be quickly implemented by a designer faced with the task of choosing a value for the ID of a hollow cylinder to be used as a roller in a friction drive.

An important factor when determining the ideal hollowness for rollers in an application is the relationship between the stress in the roller under cyclical load and the fatigue life of the roller. Further research is needed to explore this relationship. But, if it is assumed that Von Mises stress has a measurable correlation to fatigue life, and a fatigue exponent of 8 is assumed, the 12% stress reduction seen when a solid roller is replaced by one of "ideal" hollowness would lead to a fatigue life 2.8 times longer than that seen with the solid roller.

Another possible area of further research is the addition of traction forces to the analysis performed in this work. Traction adds complexity to the problem, and optimization of the hollowness of the rollers in a friction drive would be impacted.

In conclusion, the possible life improvement resulting in optimizing roller design using the method developed in this work can lead to important opportunities to use rollers in applications where they currently are not as feasible. The method can be further developed by expanding the method to include the effects of traction forces, and further investigation into the relationship between life and the stress conditions in the hollow roller.

6 REFERENCES

[1] Bowen, W. L., and Bhateja, C.P., The Hollow Roller Bearing. ASME Journal of Lubrication Technology, Vol. 102, pp. 222-228, 1980.

[2] Zhao, H., Analysis of Load Distributions Within Solid and Hollow Roller Bearings. ASME Journal of Tribology, Vol. 120, pp. 134-139, 1998

[3] Hertz, H., On the Contact of Elastic Solids. J. Reine Angew. Math., Vol. 92, pp. 156-171, 1881

[4] Murthy, C. S. C., and Rao, A. R., Mechanics and Behaviour of Hollow Cylindrical Members in Rolling Contact. Wear, Vol. 87, pp. 287-296, 1983

[5] Nelson, C. W., Stresses and Displacements in a Hollow Circular Cylinder. Ph.D. thesis, University of Michigan, 1939.

[6] Durelli, A. J., and Lin, Y. H., Stresses and Displacements on the Boundaries of Circular Rings Diametrically Loaded. Journal of Applied Mechanics, 1986.

[7] Berenberg B., St. Venant's Principle. http://plastics.about.com/library/glossary/s/bldef-s4692.htm, accessed 10 Nov. 2003. About, Inc. Copyright 2003

[8] Young, W. C., Roark's Formulas for Stress and Strain (6th Ed.)., McGraw-Hill, 1989

[9] Avoallone, E., and Baumeister, T., Mark's Standard Handbook for Mechanical Engineers. McGraw-Hill, 1996

[10] Boresi, A., Sidebottom, O., Seely, F., and Smith, J., Advanced Mechanics of Materials (3rd Ed.)., John Wiley and Sons, 1978

[11] Norton, Robert L., Machine Design, An Integrated Approach., Prentice-Hall, 1996

7 APPENDIX A: VISUAL BASIC CODE

```
Sub calcs()

' INPUT OF PARAMETERS
p = 2000 'TOTAL COMPRESSING FORCE, lb.
b = 0.5 ' OD, in.
c = 1 ' LENGTH OF CYLINDERS, in.
E = 30000000 ' MODULUS OF ELASTICITY, psi
nu = 0.3 ' POISSON'S RATIO

'OUTPUT TO SPREADSHEET, FIRST INDEX IS FOR THE ROW, THE SECOND FOR THE
'COLUMN
With Worksheets("Nelson").Cells(1, 2)
    .Value = p
End With
With Worksheets("Nelson").Cells(1, 8)
    .Value = b
End With
With Worksheets("Nelson").Cells(1, 11)
    .Value = c
End With
With Worksheets("Nelson").Cells(1, 14)
    .Value = E
End With
With Worksheets("Nelson").Cells(1, 17)
    .Value = G
End With
With Worksheets("Nelson").Cells(1, 20)
    .Value = nu
End With

'CALCULATION OF PI FOR USE THROUGHOUT THE PROGRAM
Pi = 4 * Atn(1)

'THE BELOW EQUATIONS GIVING THE CONTACT PATCH WIDTH ARE TAKEN FROM
'ROARKE'S FORMULAS FOR STRESS AND STRAIN
Kd = b * b / (b + b)
halfwidth = 2.15 * Sqr(p / c * Kd / E) / 2 ' HALF THE CONTACT PATCH WIDTH,
'IN INCHES
With Worksheets("Nelson").Cells(3, 5)
    .Value = halfwidth
End With
psi = 2 _
    * Atn((halfwidth / b) / Sqr(-(halfwidth / b) * (halfwidth / b) + 1))
'CONTACT PATCH WIDTH, IN RADIANS
With Worksheets("Nelson").Cells(3, 8)
    .Value = psi
End With

'CALCULATIONS BASED ON NELSON'S WORK, USING THE CONTACT PATCH WIDTH
'CALCULATED ABOVE

'CALCULATION INPUTS
minsearchres = 8 'PARAMETER DETERMINING RESOLUTION OF SEARCH FOR MIN
'VON MISES STRESS (HIGHER NUMBER MEANS MORE ACCURATE RESULT)
res = 18 'NUMBER OF POINTS ANALYZED IN THE ANGLE OF ANALYSIS(MUST BE EVEN)
'IF THIS NUMBER IS CHANGED, THE CELLS IN WHICH THE OUTPUT IS WRITTEN
'CHANGE, NECESSITATING EDITING THE GRAPH
locs = 25 'NUMBER OF POINTS ANALYZED IN THE DEPTH OF THE CYLINDER IF THIS
'NUMBER IS CHANGED, THE CELLS IN WHICH THE OUTPUT IS WRITTEN CHANGE,
'NECESSITATING EDITING THE GRAPH
iter = 100 'NUMBER OF TERMS IN EACH TAYLOR SERIES

qq = 3 * p / c / (2 * psi * b) ' MEASURE OF MAGNITUDE OF PARABOLIC
'PRESSURE, psi.
```

```
beta = qq * psi / 3 / Pi ' psi

'VARIABLE INITIALIZATION
repeatflag = 0
Kovm_min = 999999999
Dim lambda(201)
Dim Q(201)
Dim H(201)
Dim Hprime(201)
Dim L(201)
Dim Lprime(201)
Dim sra0_term(18)
Dim sta0_term(18)
Dim u_a0_term1(18)
Dim u_a0_term2(18)
Dim sr_eventerm(18)
Dim st_eventerm(18)
Dim u_eventerm1(18)
Dim u_eventerm2(18)
Dim sr_oddterm(18)
Dim st_oddterm(18)
Dim u_oddterm1(18)
Dim u_oddterm2(18)
line1:
'SETS a TO NEXT VALUE, IN COARSE INCREMENTS THE FIRST TIME THROUGH
'WHEN repeatflag IS ZERO, THEN IN FINE INCREMENTS THE SECOND TIME
For i = 1 To minsearchres
    If repeatflag = 0 Then
        a = 0.9 * b / minsearchres * i
    Else
        a = a_star - 0.9 * b / minsearchres + _
        2 * 0.9 * b / minsearchres / (minsearchres + 1) * i
    End If
line2:
    With Worksheets("Nelson").Cells(1, 5)
        .Value = a
    End With
    alpha = a / b ' MEASURE OF HOLLOWNESS
    For n = 1 To 2 * iter + 1
        lambda(n) = 24 / n ^ 3 / psi ^ 3 * (Sin(n * psi / 2) _
            - n * psi / 2 * Cos(n * psi / 2))
        Q(n) = (1 - alpha ^ (2 * n)) ^ 2 _
            - n ^ 2 * alpha ^ (2 * n - 2) * (1 - alpha ^ 2) ^ 2
        H(n) = n ^ 2 * (1 - alpha ^ 2) ^ 2 _
            + n * alpha ^ 2 * (1 - alpha ^ 2) _
            + alpha ^ 2 * (1 - alpha ^ (2 * n))
        Hprime(n) = n ^ 2 * (1 - alpha ^ 2) ^ 2 _
            + n * (1 - alpha ^ 2) + alpha ^ 2 * (1 - alpha ^ (2 * n))
        L(n) = n * (1 - alpha ^ 2) + (1 - alpha ^ (2 * n))
        Lprime(n) = n * (1 - alpha ^ 2) + alpha ^ 2 * (1 - alpha ^ (2 * n))
    Next

    For j = 0 To locs - 1
        r = a + (j + 1 / 2) * (b - a) / locs ' DEPTH LOCATION IN CYLINDER, in.
        With Worksheets("Nelson").Cells(j + 7, 4)
            .Value = r
        End With
        With Worksheets("Nelson").Cells(j + locs + 10, 4)
            .Value = r
        End With
        For m = 1 To res
        ' CALCULATING ANGULAR LOCATION IN CYLINDER, rad.
            If m > res / 2 Then
            theta = (m - (res / 2 + 1)) * (Pi / 2 / (res / 2 - 1)) ' ANGULAR
            'LOCATION IN CYLINDER, rad.
            Else
            theta = -Pi / 2 + (m - 1) * (Pi / 2 / (res / 2 - 1))
            End If
            sra0_term(m) = 0
            sta0_term(m) = 0
```

```
u_a0_term1(m) = 0
u_a0_term2(m) = 0
sr_eventerm(m) = 0
st_eventerm(m) = 0
u_eventerm1(m) = 0
u_eventerm2(m) = 0
sr_oddterm(m) = 0
st_oddterm(m) = 0
u_oddterm1(m) = 0
u_oddterm2(m) = 0
' CALCULATING TERMS NEEDED FOR TAYLOR SERIES CALCULATION
For k = 1 To iter
    n = 2 * k
    sra0_term(m) = sra0_term(m) _
        + (-1) ^ (n / 2) * lambda(n) * (n * (r / b) ^ (n - 2) _
        - (n - 2) * (r / b) ^ n) * Cos(n * theta)
    sta0_term(m) = sta0_term(m) _
        + (-1) ^ (n / 2) * lambda(n) * (n * (r / b) ^ (n - 2) _
        - (n + 2) * (r / b) ^ n) * Cos(n * theta)
    u_a0_term1(m) = u_a0_term1(m) _
        + (-1) ^ (n / 2) * lambda(n) * (n / (n - 1) _
        * (r / b) ^ (n - 2) - (n - 2) / (n + 1) * (r / b) ^ n) _
        * Cos(n * theta)
    u_a0_term2(m) = u_a0_term2(m) _
        + (-1) ^ (n / 2) * lambda(n) * (n / (n - 1) _
        * (r / b) ^ (n - 2) - (n + 2) / (n + 1) * (r / b) ^ n) _
        * Cos(n * theta)
    sr_eventerm(m) = sr_eventerm(m) _
        + (-1) ^ (n / 2) * lambda(n) / Q(n) * (n * H(n) _
        * alpha ^ (2 * n - 2) * (r / b) ^ (n - 2) _
        - (n - 2) * Hprime(n) * alpha ^ (2 * n - 2) _
        * (r / b) ^ n + n * L(n) * alpha ^ (2 * n) _
        * (r / b) ^ ((-n - 2) / 2) * (r / b) ^ ((-n - 2) / 2) _
        - (n + 2) * Lprime(n) * alpha ^ (2 * n - 2) _
        * (r / b) ^ (-n / 2) * (r / b) ^ (-n / 2)) _
        * Cos(n * theta)
    st_eventerm(m) = st_eventerm(m) _
        + (-1) ^ (n / 2) * lambda(n) / Q(n) * (n * H(n) _
        * alpha ^ (2 * n - 2) * (r / b) ^ (n - 2) _
        - (n + 2) * Hprime(n) * alpha ^ (2 * n - 2) _
        * (r / b) ^ n + n * L(n) * alpha ^ (2 * n) _
        * (r / b) ^ ((-n - 2) / 2) * (r / b) ^ ((-n - 2) / 2) _
        - (n - 2) * Lprime(n) * alpha ^ (2 * n - 2) _
        * (r / b) ^ (-n / 2) * (r / b) ^ (-n / 2)) _
        * Cos(n * theta)
    u_eventerm1(m) = u_eventerm1(m) _
        + (-1) ^ (n / 2) * lambda(n) / Q(n) * (n / (n - 1) _
        * H(n) * alpha ^ (2 * n - 2) * (r / b) ^ (n - 2) _
        - (n - 2) / (n + 1) * Hprime(n) * alpha ^ (2 * n - 2) _
        * (r / b) ^ n - n / (n + 1) * L(n) * alpha ^ (2 * n) _
        * (r / b) ^ ((-n - 2) / 2) * (r / b) ^ ((-n - 2) / 2) _
        + (n + 2) / (n - 1) * Lprime(n) * alpha ^ (2 * n - 2) _
        * (r / b) ^ (-n / 2) * (r / b) ^ (-n / 2)) _
        * Cos(n * theta)
    u_eventerm2(m) = u_eventerm2(m) _
        + (-1) ^ (n / 2) * lambda(n) / Q(n) * (n / (n - 1) _
        * H(n) * alpha ^ (2 * n - 2) * (r / b) ^ (n - 2) _
        - (n + 2) / (n + 1) * Hprime(n) * alpha ^ (2 * n - 2) _
        * (r / b) ^ n - n / (n + 1) * L(n) * alpha ^ (2 * n) _
        * (r / b) ^ ((-n - 2) / 2) * (r / b) ^ ((-n - 2) / 2) _
        + (n - 2) / (n - 1) * Lprime(n) * alpha ^ (2 * n - 2) _
        * (r / b) ^ (-n / 2) * (r / b) ^ (-n / 2)) _
        * Cos(n * theta)
    n = n + 1
    sr_oddterm(m) = sr_oddterm(m) _
        + (-1) ^ ((n + 1) / 2) * lambda(n) / Q(n) _
        * (n * H(n) * alpha ^ (2 * n - 2) * (r / b) ^ (n - 2) _
        - (n - 2) * Hprime(n) * alpha ^ (2 * n - 2) _
        * (r / b) ^ n + n * L(n) * alpha ^ (2 * n) _
        * (r / b) ^ ((-n - 2) / 2) * (r / b) ^ ((-n - 2) / 2) _
```

```
            - (n + 2) * Lprime(n) * alpha ^ (2 * n - 2) _
            * (r / b) ^ (-n / 2) * (r / b) ^ (-n / 2)) _
            * Sin(n * theta)
        st_oddterm(m) = st_oddterm(m) _
            + (-1) ^ ((n + 1) / 2) * lambda(n) / Q(n) _
            * (n * H(n) * alpha ^ (2 * n - 2) * (r / b) ^ (n - 2) _
            - (n + 2) * Hprime(n) * alpha ^ (2 * n - 2) _
            * (r / b) ^ n + n * L(n) * alpha ^ (2 * n) _
            * (r / b) ^ ((-n - 2) / 2) * (r / b) ^ ((-n - 2) / 2) _
            - (n - 2) * Lprime(n) * alpha ^ (2 * n - 2) _
            * (r / b) ^ (-n / 2) * (r / b) ^ (-n / 2)) _
            * Sin(n * theta)
        u_oddterm1(m) = u_oddterm1(m) _
            + (-1) ^ ((n + 1) / 2) * lambda(n) / Q(n) _
            * (n / (n - 1) * H(n) * alpha ^ (2 * n - 2) _
            * (r / b) ^ (n - 2) - (n - 2) / (n + 1) * Hprime(n) _
            * alpha ^ (2 * n - 2) * (r / b) ^ n - n / (n + 1) _
            * L(n) * alpha ^ (2 * n) * (r / b) ^ ((-n - 2) / 2) _
            * (r / b) ^ ((-n - 2) / 2) + (n + 2) / (n - 1) _
            * Lprime(n) * alpha ^ (2 * n - 2) * (r / b) ^ (-n / 2) _
            * (r / b) ^ (-n / 2)) * Sin(n * theta)
        u_oddterm2(m) = u_oddterm2(m) _
            + (-1) ^ ((n + 1) / 2) * lambda(n) / Q(n) _
            * (n / (n - 1) * H(n) * alpha ^ (2 * n - 2) _
            * (r / b) ^ (n - 2) - (n + 2) / (n + 1) * Hprime(n) _
            * alpha ^ (2 * n - 2) * (r / b) ^ n - n / (n + 1) _
            * L(n) * alpha ^ (2 * n) * (r / b) ^ ((-n - 2) / 2) _
            * (r / b) ^ ((-n - 2) / 2) + (n - 2) / (n - 1) _
            * Lprime(n) * alpha ^ (2 * n - 2) * (r / b) ^ (-n / 2) _
            * (r / b) ^ (-n / 2)) * Sin(n * theta)
    Next
    With Worksheets("Nelson").Cells(6, m + 4)
        .Value = theta
    End With
    With Worksheets("Nelson").Cells(locs + 9, m + 4)
        .Value = theta
    End With
Next
For m = 1 To res
    sra0 = -2 * beta * (1 + sra0_term(m)) ' RADIAL STRESS IN
    'HYPOTHETICAL SOLID CYLINDER, psi
    ' [NELSON (210)]
    sta0 = -2 * beta * (1 - sta0_term(m)) ' BENDING STRESS IN
    'HYPOTHETICAL SOLID CYLINDER, psi
    ' [NELSON (211)]
    u_a0 = -2 * beta * r / E * (1 + u_a0_term1(m)) _
        + 2 * nu * beta * r / E * (1 - u_a0_term2(m))
    ' [NELSON (213)]

    ' ADDITIONAL RADIAL STRESS DUE TO HOLLOWNESS, psi
    srh = -beta * (alpha ^ 2) _
        / (1 - alpha ^ 2) * (1 - b ^ 2 / r ^ 2) _
        - beta * sr_eventerm(m) + beta * sr_oddterm(m) _
        - beta * (alpha ^ 2) / (1 - alpha ^ 2) * (1 - b ^ 2 / r ^ 2) _
        - beta * sr_eventerm(res + 1 - m) _
        + beta * sr_oddterm(res + 1 - m)
    ' [NELSON (221)]
    ' ADDITIONAL BENDING STRESS DUE TO HOLLOWNESS, psi
    sth = -beta * (alpha ^ 2) / _
        (1 - alpha ^ 2) * (1 + b ^ 2 / r ^ 2) _
        + beta * st_eventerm(m) - beta * st_oddterm(m) _
        - beta * (alpha ^ 2) / (1 - alpha ^ 2) * (1 + b ^ 2 / r ^ 2) _
        + beta * st_eventerm(res + 1 - m) _
        - beta * st_oddterm(res + 1 - m)
    ' [NELSON (222)]
    u_h = -beta * r / E * (alpha ^ 2 _
        / (1 - alpha ^ 2) * (1 + b ^ 2 / r ^ 2) + u_eventerm1(m) _
        - u_oddterm1(m)) + nu * beta * r / E * (alpha ^ 2 _
        / (1 - alpha ^ 2) * (1 - b ^ 2 / r ^ 2) - u_eventerm2(m) _
        + u_oddterm2(m)) - beta * r / E _
```

```
                * (alpha ^ 2 / (1 - alpha ^ 2) * (1 + b ^ 2 / r ^ 2) _
                + u_eventerm1(res + 1 - m) - u_oddterm1(res + 1 - m)) _
                + nu * beta * r / E * (alpha ^ 2 / (1 - alpha ^ 2) _
                * (1 - b ^ 2 / r ^ 2) - u_eventerm2(res + 1 - m) _
                + u_oddterm2(res + 1 - m))
            ' [NELSON (224)]

            ' TOTAL RADIAL STRESS, psi
            sr = sra0 + srh
            ' TOTAL BENDING STRESS, psi
            st = sta0 + sth
            u = -2 * (u_a0 + u_h)

            ' RADIAL STRESS IN TERMS OF STRESS FACTOR
            Kor = sr / (p / (Pi * b * c))
            ' BENDING STRESS IN TERMS OF STRESS FACTOR
            Kot = st / (p / (Pi * b * c))
            ' AXIAL STRESS IN TERMS OF STRESS FACTOR
            Koa = nu * Kor + nu * Kot
            ' VON MISES STRESS IN TERMS OF STRESS FACTOR
            Kovm = 1 / (2 ^ 0.5) _
                 * ((Kor - Kot) ^ 2 + (Kor - Koa) ^ 2 + (Kot - Koa) ^ 2) ^ 0.5
            With Worksheets("Nelson").Cells(j + 7, m + 4)
                .Value = Kot
            End With
            With Worksheets("Nelson").Cells(j + locs + 10, m + 4)
                .Value = Kor
            End With
            With Worksheets("Nelson").Cells(j + 2 * locs + 13, m + 4)
                .Value = Koa
            End With
            With Worksheets("Nelson").Cells(j + 3 * locs + 16, m + 4)
                .Value = Kovm
            End With
            If j = locs - 1 Then
                If m = 1 Then
                    With Worksheets("Nelson").Cells(3, 17)
                        .Value = u
                    End With
                End If
            End If
        Next
    Next
    If Worksheets("Nelson").Cells(3, 11).Value <= Kovm_min Then
        Kovm_min = Worksheets("Nelson").Cells(3, 11).Value
        If repeatflag = 0 Then
            a_star = a
        Else
            a_star_star = a
        End If
    End If
    If repeatflag = 2 Then GoTo line4
Next
'NAVIGATION RUNNING THE PROGRAM THROUGH THE SEARCH FOR MINIMUM STRESS
'FACTOR.  repeatflag = 0 THE FIRST TIME, 1 THE SECOND TIME, and 2 THE
'FINAL TIME WHEN IT DOES THE CALCULATION OVER FOR THE OPTIMUM VALUE
If repeatflag = 1 Then GoTo line3
repeatflag = 1
GoTo line1
line3:
repeatflag = 2
a = a_star_star
GoTo line2
line4:

End Sub
```

8 APPENDIX B: TABULAR DATA

Table 8.1, Visual Basic Program Output, Bending Stress at Optimum Hollowness

σ_θ				K^0_θ								
				-1.57	-1.37	-1.18	-0.98	-0.79	-0.59	-0.39	-0.20	0.00
Normalized Depth, z' = (b-z)/(b-a)	z'=0.98	Location In Depth of Material	0.3795	86.3	62.9	33.4	7.4	-15.4	-34.1	-47.9	-56.5	-59.4
	z'=0.94		0.3844	76.6	56.4	29.9	6.4	-14.2	-31.1	-43.6	-51.3	-53.9
	z'=0.90		0.3893	67.5	50.0	26.4	5.4	-13.1	-28.2	-39.4	-46.4	-48.7
	z'=0.86		0.3942	59.1	43.8	23.1	4.4	-12.0	-25.4	-35.4	-41.5	-43.6
	z'=0.82		0.3991	51.2	37.7	19.8	3.4	-11.0	-22.7	-31.5	-36.9	-38.7
	z'=0.78		0.4041	43.7	31.9	16.5	2.4	-10.0	-20.2	-27.7	-32.4	-33.9
	z'=0.74		0.4090	36.7	26.1	13.4	1.4	-9.1	-17.7	-24.1	-28.0	-29.3
	z'=0.70		0.4139	30.0	20.6	10.3	0.5	-8.2	-15.2	-20.5	-23.7	-24.8
	z'=0.66		0.4188	23.5	15.2	7.3	-0.5	-7.3	-12.9	-17.0	-19.6	-20.5
	z'=0.62		0.4237	17.3	10.0	4.4	-1.4	-6.4	-10.6	-13.7	-15.6	-16.2
	z'=0.58		0.4287	11.3	4.9	1.5	-2.3	-5.6	-8.4	-10.4	-11.6	-12.1
	z'=0.54		0.4336	5.5	-0.1	-1.3	-3.2	-4.8	-6.2	-7.2	-7.8	-8.0
	z'=0.50		0.4385	-0.1	-4.9	-4.1	-4.0	-4.1	-4.1	-4.1	-4.1	-4.1
	z'=0.46		0.4434	-5.6	-9.6	-6.8	-4.9	-3.3	-2.0	-1.0	-0.4	-0.2
	z'=0.42		0.4483	-11.0	-14.1	-9.4	-5.7	-2.5	0.1	2.0	3.2	3.6
	z'=0.38		0.4533	-16.3	-18.5	-11.9	-6.5	-1.8	2.1	4.9	6.7	7.3
	z'=0.34		0.4582	-21.5	-22.7	-14.4	-7.3	-1.1	4.0	7.8	10.2	11.0
	z'=0.30		0.4631	-26.6	-26.9	-16.9	-8.1	-0.4	6.0	10.7	13.6	14.5
	z'=0.26		0.4680	-31.8	-30.9	-19.3	-8.8	0.4	7.9	13.5	16.9	18.1
	z'=0.22		0.4729	-36.9	-34.7	-21.6	-9.5	1.1	9.8	16.2	20.2	21.5
	z'=0.18		0.4779	-42.0	-38.5	-23.9	-10.2	1.8	11.6	18.9	23.4	24.9
	z'=0.14		0.4828	-47.5	-42.1	-26.1	-10.9	2.5	13.4	21.6	26.6	28.3
	z'=0.10		0.4877	-54.4	-45.6	-28.3	-11.6	3.2	15.3	24.2	29.8	31.6
	z'=0.06		0.4926	-69.1	-48.9	-30.5	-12.3	3.9	17.1	26.8	32.9	35.0
	z'=0.02		0.4975	-134.2	-52.8	-32.6	-12.8	4.6	18.8	29.4	35.9	38.1

The data in the table above is plotted in Figure 4.1.

Table 8.2, Visual Basic Program Output, Radial Stress at Optimum Hollowness

σ_r				K^0_r								
				-1.57	-1.37	-1.18	-0.98	-0.79	-0.59	-0.39	-0.20	0.00
Normalized Depth, z' = (b-z)/(b-a)	z'=0.98	Location In Depth of Material	0.3795	0.5	0.4	0.2	0.1	-0.1	-0.2	-0.3	-0.4	-0.4
	z'=0.94		0.3844	1.3	1.2	0.6	0.2	-0.3	-0.6	-0.9	-1.0	-1.1
	z'=0.90		0.3893	1.6	1.9	1.0	0.2	-0.4	-0.9	-1.3	-1.6	-1.7
	z'=0.86		0.3942	1.7	2.5	1.3	0.3	-0.5	-1.2	-1.7	-2.1	-2.2
	z'=0.82		0.3991	1.4	2.9	1.6	0.4	-0.6	-1.4	-2.1	-2.4	-2.6
	z'=0.78		0.4041	1.0	3.4	1.9	0.5	-0.7	-1.6	-2.3	-2.7	-2.9
	z'=0.74		0.4090	0.3	3.7	2.1	0.6	-0.7	-1.7	-2.5	-3.0	-3.1
	z'=0.70		0.4139	-0.6	3.9	2.2	0.6	-0.7	-1.8	-2.6	-3.2	-3.3
	z'=0.66		0.4188	-1.6	4.1	2.4	0.7	-0.7	-1.9	-2.7	-3.3	-3.4
	z'=0.62		0.4237	-2.8	4.3	2.5	0.7	-0.7	-1.9	-2.8	-3.3	-3.5
	z'=0.58		0.4287	-4.2	4.3	2.5	0.8	-0.7	-1.9	-2.8	-3.3	-3.5
	z'=0.54		0.4336	-5.8	4.3	2.5	0.8	-0.7	-1.9	-2.8	-3.3	-3.5
	z'=0.50		0.4385	-7.6	4.3	2.5	0.8	-0.6	-1.8	-2.7	-3.2	-3.4
	z'=0.46		0.4434	-9.6	4.2	2.5	0.8	-0.6	-1.7	-2.6	-3.1	-3.3
	z'=0.42		0.4483	-12.0	4.1	2.4	0.8	-0.6	-1.6	-2.5	-3.0	-3.1
	z'=0.38		0.4533	-14.7	3.9	2.3	0.8	-0.5	-1.5	-2.3	-2.8	-2.9
	z'=0.34		0.4582	-17.9	3.7	2.1	0.7	-0.5	-1.4	-2.1	-2.6	-2.7
	z'=0.30		0.4631	-21.7	3.4	2.0	0.7	-0.4	-1.3	-1.9	-2.4	-2.5
	z'=0.26		0.4680	-26.5	3.1	1.8	0.6	-0.3	-1.1	-1.7	-2.1	-2.2
	z'=0.22		0.4729	-32.8	2.7	1.5	0.6	-0.3	-1.0	-1.5	-1.8	-1.9
	z'=0.18		0.4779	-41.4	2.3	1.3	0.5	-0.2	-0.8	-1.3	-1.5	-1.6
	z'=0.14		0.4828	-54.2	1.8	1.1	0.4	-0.2	-0.7	-1.0	-1.2	-1.3
	z'=0.10		0.4877	-74.7	1.2	0.8	0.3	-0.2	-0.5	-0.7	-0.9	-1.0
	z'=0.06		0.4926	-110.1	0.1	0.6	0.4	-0.2	-0.4	-0.3	-0.5	-0.7
	z'=0.02		0.4975	-164.2	-2.4	0.7	0.9	-0.6	-0.5	0.4	-0.1	-0.7

The data in the table above is plotted in Figure 4.2.

Table 8.3, Visual Basic Program Output, Axial Stress at Optimum Hollowness

σ_a				K^0_a								
				-1.57	-1.37	-1.18	-0.98	-0.79	-0.59	-0.39	-0.20	0.00
Normalized Depth, z' = (b-z)/(b-a)	z'=0.98	Location In Depth of Material	0.3795	26.1	19.0	10.1	2.2	-4.6	-10.3	-14.5	-17.1	-17.9
	z'=0.94		0.3844	23.3	17.3	9.1	2.0	-4.3	-9.5	-13.3	-15.7	-16.5
	z'=0.90		0.3893	20.7	15.6	8.2	1.7	-4.0	-8.7	-12.2	-14.4	-15.1
	z'=0.86		0.3942	18.2	13.9	7.3	1.4	-3.8	-8.0	-11.1	-13.1	-13.7
	z'=0.82		0.3991	15.8	12.2	6.4	1.1	-3.5	-7.3	-10.1	-11.8	-12.4
	z'=0.78		0.4041	13.4	10.6	5.5	0.9	-3.2	-6.5	-9.0	-10.5	-11.1
	z'=0.74		0.4090	11.1	8.9	4.6	0.6	-2.9	-5.8	-8.0	-9.3	-9.7
	z'=0.70		0.4139	8.8	7.4	3.8	0.3	-2.7	-5.1	-6.9	-8.1	-8.4
	z'=0.66		0.4188	6.6	5.8	2.9	0.1	-2.4	-4.4	-5.9	-6.9	-7.2
	z'=0.62		0.4237	4.4	4.3	2.0	-0.2	-2.1	-3.7	-4.9	-5.7	-5.9
	z'=0.58		0.4287	2.1	2.8	1.2	-0.5	-1.9	-3.1	-4.0	-4.5	-4.7
	z'=0.54		0.4336	-0.1	1.3	0.4	-0.7	-1.6	-2.4	-3.0	-3.3	-3.5
	z'=0.50		0.4385	-2.3	-0.2	-0.5	-1.0	-1.4	-1.8	-2.0	-2.2	-2.2
	z'=0.46		0.4434	-4.6	-1.6	-1.3	-1.2	-1.2	-1.1	-1.1	-1.1	-1.0
	z'=0.42		0.4483	-6.9	-3.0	-2.1	-1.5	-0.9	-0.5	-0.1	0.1	0.1
	z'=0.38		0.4533	-9.3	-4.4	-2.9	-1.7	-0.7	0.2	0.8	1.2	1.3
	z'=0.34		0.4582	-11.8	-5.7	-3.7	-2.0	-0.5	0.8	1.7	2.3	2.5
	z'=0.30		0.4631	-14.5	-7.0	-4.5	-2.2	-0.2	1.4	2.6	3.4	3.6
	z'=0.26		0.4680	-17.5	-8.3	-5.3	-2.5	0.0	2.0	3.5	4.4	4.8
	z'=0.22		0.4729	-20.9	-9.6	-6.0	-2.7	0.2	2.6	4.4	5.5	5.9
	z'=0.18		0.4779	-25.0	-10.9	-6.8	-2.9	0.5	3.2	5.3	6.6	7.0
	z'=0.14		0.4828	-30.5	-12.1	-7.5	-3.2	0.7	3.8	6.2	7.6	8.1
	z'=0.10		0.4877	-38.7	-13.3	-8.3	-3.4	0.9	4.4	7.1	8.7	9.2
	z'=0.06		0.4926	-53.8	-14.7	-9.0	-3.6	1.1	5.0	7.9	9.7	10.3
	z'=0.02		0.4975	-89.5	-16.6	-9.6	-3.6	1.2	5.5	8.9	10.8	11.2

The data in the table above is plotted in Figure 4.3.

Table 8.4, Visual Basic Program Output, Von Mises Stress at Optimum Hollowness

σ_{vm}				K^0_{vm}								
				-1.57	-1.37	-1.18	-0.98	-0.79	-0.59	-0.39	-0.20	0.00
Normalized Depth, z' = (b-z)/(b-a)	0.98	Location In Depth of Material	0.3795	76.3	55.6	29.5	6.5	13.6	30.1	42.4	49.9	52.5
	0.94		0.3844	67.0	49.2	26.0	5.5	12.4	27.1	38.1	44.8	47.1
	0.90		0.3893	58.7	42.9	22.7	4.6	11.3	24.3	34.0	39.9	41.9
	0.86		0.3942	51.2	37.0	19.4	3.6	10.3	21.6	30.1	35.3	37.0
	0.82		0.3991	44.4	31.2	16.3	2.7	9.3	19.1	26.4	30.8	32.4
	0.78		0.4041	38.1	25.7	13.2	1.7	8.4	16.7	22.8	26.6	27.9
	0.74		0.4090	32.4	20.3	10.3	0.8	7.5	14.3	19.4	22.5	23.6
	0.70		0.4139	27.1	15.2	7.4	0.3	6.7	12.1	16.1	18.6	19.5
	0.66		0.4188	22.2	10.3	4.7	1.0	5.9	10.0	13.0	14.9	15.5
	0.62		0.4237	17.7	5.7	2.1	1.8	5.2	7.9	10.0	11.3	11.7
	0.58		0.4287	13.5	1.9	1.2	2.7	4.5	6.0	7.1	7.8	8.0
	0.54		0.4336	9.8	3.9	3.3	3.5	3.8	4.1	4.3	4.5	4.6
	0.50		0.4385	6.7	8.0	5.7	4.2	3.1	2.3	1.8	1.6	1.6
	0.46		0.4434	4.6	12.0	8.0	5.0	2.5	0.8	1.6	2.5	2.8
	0.42		0.4483	4.7	15.9	10.3	5.7	1.8	1.5	3.9	5.3	5.8
	0.38		0.4533	6.3	19.6	12.4	6.4	1.2	3.1	6.3	8.3	8.9
	0.34		0.4582	8.5	23.2	14.5	7.1	0.6	4.8	8.7	11.1	12.0
	0.30		0.4631	10.6	26.6	16.6	7.7	0.2	6.4	11.1	14.0	14.9
	0.26		0.4680	12.5	29.9	18.5	8.3	0.6	7.9	13.4	16.7	17.9
	0.22		0.4729	14.4	33.0	20.4	8.9	1.2	9.5	15.6	19.4	20.7
	0.18		0.4779	16.7	36.0	22.3	9.5	1.8	11.0	17.8	22.0	23.5
	0.14		0.4828	21.1	38.9	24.1	10.0	2.3	12.5	20.0	24.6	26.2
	0.10		0.4877	31.3	41.5	25.8	10.6	3.0	14.0	22.1	27.2	28.9
	0.06		0.4926	50.5	43.5	27.6	11.2	3.7	15.5	24.0	29.6	31.7
	0.02		0.4975	65.1	45.0	29.5	12.1	4.5	17.1	25.8	32.0	34.5

The data in the table above is plotted in Figure 4.4.

Table 8.5, Spreadsheet Calculation, Bending Stress at Optimum Hollowness

σ_θ				K^0_θ								
				-1.57	-1.37	-1.18	-0.98	-0.79	-0.59	-0.39	-0.20	0.00
Normalized Depth, z' = (b-z)/(b-a)	z'=0.98	Location In Depth of Material	0.3795	90.7	61.4	33.4	7.5	-15.2	-33.8	-47.7	-56.2	-59.1
	z'=0.94		0.3844	81.7	55.2	29.8	6.4	-14.2	-31.0	-43.5	-51.2	-53.8
	z'=0.90		0.3893	72.9	49.2	26.3	5.3	-13.1	-28.2	-39.5	-46.4	-48.7
	z'=0.86		0.3942	64.3	43.2	23.0	4.3	-12.1	-25.6	-35.5	-41.7	-43.8
	z'=0.82		0.3991	56.0	37.5	19.7	3.3	-11.1	-22.9	-31.7	-37.1	-38.9
	z'=0.78		0.4041	47.8	31.8	16.4	2.3	-10.2	-20.4	-27.9	-32.6	-34.2
	z'=0.74		0.4090	39.9	26.3	13.3	1.3	-9.2	-17.9	-24.3	-28.2	-29.6
	z'=0.70		0.4139	32.1	21.0	10.2	0.4	-8.3	-15.4	-20.7	-24.0	-25.1
	z'=0.66		0.4188	24.6	15.7	7.3	-0.6	-7.4	-13.0	-17.2	-19.8	-20.7
	z'=0.62		0.4237	17.2	10.6	4.3	-1.5	-6.5	-10.7	-13.8	-15.7	-16.4
	z'=0.58		0.4287	9.9	5.6	1.5	-2.3	-5.7	-8.4	-10.5	-11.7	-12.2
	z'=0.54		0.4336	2.9	0.7	-1.3	-3.2	-4.9	-6.2	-7.2	-7.8	-8.1
	z'=0.50		0.4385	-4.0	-4.0	-4.0	-4.0	-4.0	-4.0	-4.0	-4.0	-4.0
	z'=0.46		0.4434	-10.8	-8.7	-6.7	-4.9	-3.2	-1.9	-0.9	-0.3	-0.1
	z'=0.42		0.4483	-17.4	-13.3	-9.3	-5.7	-2.5	0.2	2.1	3.3	3.7
	z'=0.38		0.4533	-23.9	-17.7	-11.9	-6.4	-1.7	2.2	5.1	6.9	7.5
	z'=0.34		0.4582	-30.2	-22.1	-14.4	-7.2	-1.0	4.2	8.0	10.4	11.2
	z'=0.30		0.4631	-36.4	-26.4	-16.8	-8.0	-0.2	6.1	10.9	13.8	14.8
	z'=0.26		0.4680	-42.4	-30.6	-19.2	-8.7	0.5	8.0	13.7	17.1	18.3
	z'=0.22		0.4729	-48.4	-34.7	-21.5	-9.4	1.2	9.9	16.4	20.4	21.7
	z'=0.18		0.4779	-54.2	-38.7	-23.8	-10.1	1.9	11.7	19.1	23.6	25.1
	z'=0.14		0.4828	-59.9	-42.6	-26.1	-10.8	2.6	13.5	21.7	26.7	28.4
	z'=0.10		0.4877	-65.4	-46.5	-28.3	-11.5	3.2	15.3	24.3	29.8	31.6
	z'=0.06		0.4926	-70.9	-50.3	-30.4	-12.2	3.9	17.0	26.8	32.8	34.8
	z'=0.02		0.4975	-76.3	-54.0	-32.6	-12.8	4.5	18.7	29.2	35.7	37.9

The data in the table above is plotted in Figure 4.5.

Table 8.6, Von Mises Stress at Contact Point, FEA and Nelson's Equations, Varying Hollowness

	Von Mises Stress Factor At Contact Point	
Hollowness	Nelson	FEA
0.010	77.2	73.5
0.450	93.2	71.2
0.600	87.8	67.5
0.650	82.2	
0.700	74.1	
0.754	65.1	64.4
0.800	73.5	
0.850	148.1	
0.900	413.0	402.3

The data in the table above is plotted in Figure 4.6.

Table 8.7, FEA, Von Mises Stress at Optimum Hollowness

σ_{vm}				K^0_{vm}	
				-1.57	0.00
Normalized Depth, z' = (b-z)/(b-a)	0.98	Location In Depth of Material	0.3794	78.3	54.0
	0.94		0.3843	68.7	48.6
	0.90		0.3892	60.0	43.4
	0.86		0.3941	52.3	38.4
	0.82		0.3990	45.2	33.7
	0.78		0.4039	38.8	29.1
	0.74		0.4089	32.9	24.8
	0.70		0.4138	27.6	20.6
	0.66		0.4187	22.6	16.6
	0.62		0.4236	18.1	12.8
	0.58		0.4285	14.0	9.1
	0.54		0.4334	10.6	5.6
	0.50		0.4384	7.9	2.7
	0.46		0.4433	6.6	2.7
	0.42		0.4482	7.1	5.4
	0.38		0.4531	8.6	8.5
	0.34		0.4580	10.8	11.5
	0.30		0.4629	12.8	14.5
	0.26		0.4678	14.9	17.5
	0.22		0.4728	17.0	20.3
	0.18		0.4777	19.3	23.2
	0.14		0.4826	23.1	25.9
	0.10		0.4875	31.6	28.6
	0.06		0.4924	52.8	31.3
	0.02		0.4973	63.1	33.9

The data in the table above is plotted in Figure 4.16.

Table 8.8, FEA Data, Bending Stress at Optimum Hollowness

σ_θ				K^0_θ	
				-1.57	0.00
Normalized Depth, z' = (b-z)/(b-a)	0.98	Location In Depth of Material	0.3794	89.2	-60.8
	0.94		0.3843	79.0	-55.3
	0.90		0.3892	69.6	-50.0
	0.86		0.3941	60.9	-44.9
	0.82		0.3990	52.7	-39.9
	0.78		0.4039	45.0	-35.1
	0.74		0.4089	37.7	-30.4
	0.70		0.4138	30.8	-25.8
	0.66		0.4187	24.1	-21.4
	0.62		0.4236	17.7	-17.1
	0.58		0.4285	11.5	-12.9
	0.54		0.4334	5.6	-8.8
	0.50		0.4384	-0.3	-4.7
	0.46		0.4433	-5.9	-0.8
	0.42		0.4482	-11.5	3.0
	0.38		0.4531	-16.9	6.8
	0.34		0.4580	-22.4	10.5
	0.30		0.4629	-27.7	14.1
	0.26		0.4678	-33.1	17.7
	0.22		0.4728	-38.6	21.2
	0.18		0.4777	-43.8	24.7
	0.14		0.4826	-50.7	28.1
	0.10		0.4875	-56.9	31.5
	0.06		0.4924	-67.9	34.8
	0.02		0.4973	-154.2	38.1

The data in the table above is plotted in Figure 4.17.

Table 8.9, FEA Data, Radial Stress at Optimum Hollowness

σ_r				K^0_r	
				-1.57	0.00
Normalized Depth, z' = (b-z)/(b-a)	0.98	Location In Depth of Material	0.3794	0.5	-0.4
	0.94		0.3843	1.3	-1.1
	0.90		0.3892	1.6	-1.7
	0.86		0.3941	1.6	-2.2
	0.82		0.3990	1.4	-2.6
	0.78		0.4039	0.9	-3.0
	0.74		0.4089	0.2	-3.2
	0.70		0.4138	-0.8	-3.4
	0.66		0.4187	-1.9	-3.5
	0.62		0.4236	-3.2	-3.6
	0.58		0.4285	-4.7	-3.6
	0.54		0.4334	-6.3	-3.5
	0.50		0.4384	-8.2	-3.5
	0.46		0.4433	-10.4	-3.3
	0.42		0.4482	-12.8	-3.2
	0.38		0.4531	-15.6	-3.0
	0.34		0.4580	-19.0	-2.8
	0.30		0.4629	-22.9	-2.5
	0.26		0.4678	-28.0	-2.2
	0.22		0.4728	-33.9	-1.9
	0.18		0.4777	-42.9	-1.6
	0.14		0.4826	-54.1	-1.3
	0.10		0.4875	-73.6	-0.9
	0.06		0.4924	-110.7	-0.6
	0.02		0.4973	-151.2	-0.2

The data in the table above is plotted in Figure 4.18.

Table 8.10, FEA Data, Axial Stress at Optimum Hollowness

σ_a				K^0_a	
				-1.57	0.00
Normalized Depth, z' = (b-z)/(b-a)	0.98	Location In Depth of Material	0.3794	29.3	-17.2
	0.94		0.3843	26.4	-15.8
	0.90		0.3892	23.7	-14.4
	0.86		0.3941	21.1	-13.0
	0.82		0.3990	18.5	-11.6
	0.78		0.4039	16.0	-10.3
	0.74		0.4089	13.6	-9.0
	0.70		0.4138	11.2	-7.7
	0.66		0.4187	8.9	-6.5
	0.62		0.4236	6.6	-5.2
	0.58		0.4285	4.2	-4.0
	0.54		0.4334	1.9	-2.8
	0.50		0.4384	-0.4	-1.6
	0.46		0.4433	-2.8	-0.4
	0.42		0.4482	-5.2	0.8
	0.38		0.4531	-7.7	1.9
	0.34		0.4580	-10.4	3.1
	0.30		0.4629	-13.1	4.2
	0.26		0.4678	-16.3	5.3
	0.22		0.4728	-19.7	6.4
	0.18		0.4777	-24.0	7.6
	0.14		0.4826	-29.5	8.7
	0.10		0.4875	-37.2	9.8
	0.06		0.4924	-51.6	10.9
	0.02		0.4973	-89.7	12.0

The data in the table above is plotted in Figure 4.19.

Table 8.11, Contact Pressure Data, FEA Method, at Optimum Hollowness

Y	α=0.010	Y	α=0.450	Y	α=0.600	Y	α=0.754	Y	α=0.900
0.0000	156.0	0.0000	157.1	0.0000	159.1	0.0000	158.7	0.0000	118.3
0.0036	156.1	0.0036	157.1	0.0036	158.8	0.0036	158.1	0.0036	121.6
0.0073	133.6	0.0073	135.4	0.0073	138.8	0.0073	140.3	0.0072	111.6
0.0111	67.0	0.0111	69.2	0.0111	73.4	0.0111	76.7	0.0109	93.7
0.0150	0.0	0.0150	0.0	0.0150	0.0	0.0150	0.0	0.0147	48.6
								0.0186	0.0

The factor Y in the table above gives the distance from the center of the contact pressure distribution. The data in the table above is plotted in Figure 4.23.

Table 8.12, Displacement Data, FEA and Nelson's Equations, Varying Hollowness

	Displacement In Inches		Normalized Displacements	
Hollowness	Nelson	FEA	Nelson	FEA
0.01	0.000358	0.000423	0.000717	0.000846
0.45	0.000705	0.000706	0.00141	0.001412
0.6	0.00148	0.00142	0.00297	0.00284
0.754	0.00616	0.00577	0.0123	0.0115
0.9	0.104	0.0969	0.207	0.194

The data in the table above is plotted in Figure 4.24.

Table 8.13, Von Mises Stress at Contact Point, FEA and Nelson's Equations, Varying Hollowness

Hollowness	Bending Stress Factor At ID Below Contact Point
0.010	1.0
0.450	14.8
0.600	30.4
0.650	40.6
0.700	56.7
0.754	86.3
0.800	133.2
0.850	241.8
0.900	554.8

The data in the table above is plotted in Figure 5.2.